MULTIVARIABLE AVERAGING LEVEL CONTROL

By

Manpreet S. Sidhu

B. Sc. (Chemical Engineering) University of British Columbia, 2001

A THESIS SUBMITTED IN PARTIAL FULFILLMENT OF

THE REQUIREMENTS FOR THE DEGREE OF

MASTER OF APPLIED SCIENCE

in

THE FACULTY OF GRADUATE STUDIES

DEPARTMENT OF ELECTRICAL AND COMPUTER ENGINEERING

We accept this thesis as conforming

to the required standard

THE UNIVERSITY OF BRITISH COLUMBIA

April 2003

In presenting this thesis in partial fulfilment of the requirements for an advanced degree at the University of British Columbia, I agree that the Library shall make it freely available for reference and study. I further agree that permission for extensive copying of this thesis for scholarly purposes may be granted by the head of my department or by his or her representatives. It is understood that copying or publication of this thesis for financial gain shall not be allowed without my written permission.

Department of Electrical and Computer Engineering
The University of British Columbia
2356 Main Mall
Vancouver, Canada
V6T 1Z4

Date: April 23/03

Abstract

This thesis studies the multivariable averaging level control problem by developing and comparing various controller design techniques. Due to obvious safety and economic considerations, the level of a surge tank must never be allowed to overflow or become empty, while the flow rate constraints must be satisfied. Hence, the main emphasis of the thesis is on the study of constrained controller design techniques.

Multivariable design techniques such as decentralized, decoupled and full multivariable control are studied. The special structure of the system model allows for a constant decoupling matrix over all frequencies. This significantly simplifies the decoupled controller design. In full multivariable control, constrained Model Based Predictive Control (MPC) is utilized as it is able to naturally incorporate system constraints. Various cost function formulations which lead to either Quadratic or Linear Programming optimizations are presented and compared. The drawback of incorporating a terminal constraint set in MPC design is also studied. A novel mixed norm MPC algorithm that removes the requirement for using a terminal constraint set is proposed. MPC based on QP optimization is shown to provide the best results. The nonsmooth behaviour of MPC under LP optimization is also discussed. Finally, the practicality of some computationally-friendly techniques is assessed on a lab scale two-tank apparatus. The control algorithms are implemented in real-time using MatLab and dSpace.

Table of Contents

List of Tables

List of Figures

Acknowledgements

During the course of this thesis I have had the assistance of many people who have helped in shaping this thesis and my future.

I would like to thank my supervisor Dr. Guy Dumont for providing me this opportunity and allowing me the freedom to pursue a topic of my own interest. Thank you for your friendship and providing valuable advice on both technical and personal issues. My co-supervisor, Dr. Bruce Allison, thank you for your guidance, support and friendship. Under your supervision I was able to learn a great deal about both the technical and practical aspects of control engineering. Your dedication to your students is commendable.

Dr. Mihai Huzmezan, thank you for your friendship, humour and time to discuss my thesis on a regular basis. Your input into various topics was invaluable.

Dr. Ezra Kwok, thank you for inspiring me to pursue process control. It was your enthusiasm and dedication during my undergraduate studies that lead me in this path. Good luck in your future endeavours.

To my friends and office mates, Michael Chong Ping and Stevo Mijanovic, thank you for the lively educational and philosophical discussions. At times the office seemed too small, but I am sure we will look back at the good times. Guantien Tan, thank you for your friendship and always having the time for our discussions. I would like to thank Shiro Ogawa for his excellent suggestions and comments regarding this thesis. Shiro, your ability to question everything (well, almost everything) is truly remarkable. Also thanks to Ming Chen, Setareh Aslani, Stephane Bibian and Junqiang Fan for the interesting conversations, and thanks to the PPC and ECE adminstration and technical staff for their assistance.

Finally, I would like to thank my family. Thank you to my parents who sent me to Canada for the dream of a better education and a better life. I must especially thank my grandparents who undertook the responsibility at such an age to fulfill my parents dreams. I hope the completion of this degree is an affirmation of your hardwork and dedication. I would also like to thank my new wife and her family for their support. Thanks especially to my wife for her love, encouragement, patience and understanding.

Thanks everybody!

Chapter 1

Introduction

In the process industries, level control of a vessel can be set up to provide flow smoothing or tight level control. In some special applications, tight level control is required, such as in the level control of a Continuous Stirred Tank Reactor (CSTR), where the reactor volume is to be tightly maintained at a set value. However, the majority of tanks in a process plant serve as surge vessels where flow filtering is required. A common application of a surge vessel is the feed tank to a distillation column. For the proper operation of the distillation column, the outlet flow from the feed tank must be kept as smooth as possible.

Without loss of generality, it is assumed that the outlet flow of the tank is manipulated for level control. In order to maintain tight level control, subject to inlet flow disturbances, the tank outlet flow must be aggressively manipulated. Hence, a reduction in level variability is achieved at the expense of increasing outlet flow variability. As is common to all physical systems, the variation in the system cannot be eliminated but only redirected within the system. The optimal use of the available surge capacity of the tank to produce maximum flow filtering (or the ability to transfer variability from inlet flow to the level) is referred to as averaging level control.

Due to increased economic and environmental pressures, process plants are deploying an increasing number of recycle streams. Recycle streams introduce interactions between various unit operations, making the process a multivariable system. When recycle streams are closed around processes that contain surge vessels, the averaging level control problem becomes a multi-input multi-output (MIMO) control problem. McDonald and McAvoy [12] address a single-input single-output (SISO) averaging level control problem for a single tank. They stated that the objective of an averaging level controller is to minimize the maximum rate of change of the outlet flow rate (MRCO) for a given deterministic perturbation, while maintaining the tank within its level constraints.

As the above problem formulation suggests, the solution being sought does not lead to conventional regulatory controller synthesis. The objective of conventional regulatory control is to achieve the highest possible closed-loop bandwidth for disturbance rejection. Contrary to this, in averaging level control the objective is to obtain the smallest closed-loop bandwidth while satisfying input and output constraints. As the overflow or emptying of tanks can be disastrous, the controller's ability to handle state or output constraints is considered paramount. For both SISO and MIMO systems, the averaging level control algorithm must possess the following characteristics:

- For a given flow disturbance, the manipulated flow rate changes are minimum, i.e. minimize MRCO.
- Maximum surge capacity is utilized while maintaining the tank level within its maximum and minimum level constraints.
- The manipulated flow rate must be kept within its minimum and maximum constraints.
- After attenuating a disturbance, the tank level must be steered back to its setpoint, i.e. integral action must be present.

The remainder of this chapter first proceeds to review the field of averaging level control. The industrial system that motivated this thesis is also briefly discussed. In order to better understand the problem and to provide a convenient means of accessing various controller design techniques, a laboratory two-tank system is presented. The model equations are derived and a controllability analysis is presented.

1.1 Literature Review

The importance of averaging level control had been realized long ago, as both academic and practicing engineers attempted to provide a solution. All of the work so far, with one exception, has concentrated on controlling a single tank. In this review, the evolution from ad-hoc techniques to optimization-based methods is presented.

1.1.1 Ad-hoc methods

In this section, averaging level control methodologies for a single tank system that are based on the ad-hoc augmentation of the Proportional-Integral-Derivative (PID) algorithm are presented.

- Nonlinear PI Control presented by Shunta and Fehervari [10] incorporated gain scheduling. Using inlet flow rate as the scheduling variable, the PI controller gain was varied to accommodate varying load disturbances. Shunta and Fehervari also proposed an algorithm where both the PI gain and reset time were adjusted in an exponential manner. The switching curve was empirically determined.
- Another technique similar to [10] called Dual Range Integral/Proportional (DRIP) was proposed by Cheung and Luyben [22]. In this technique, the tank level was divided into different error bands. Within these error bands, the integral time of the PI controller was varied to obtain the desired closed-loop response.

- Proportional-Lag (PL) controller introduced by Luyben and Buckley [23] incorporates a basic P level controller with a feedforward controller. Flow into the tank is measured and transmitted through a first-order lag, which is then added to the output of the P level controller. This strategy provides the advantages of both a P controller, and a PI controller. Excellent flow filtering is obtained as with a P controller and PI controller characteristics are preserved as the off-set can be eliminated. Tuning charts are presented with respect to MRCO and the maximum peak height of the outlet flow.

- Limited Output Change (LOC) was also proposed by Cheung and Luyben [22]. This scheme limits the controller output in order to meet the MRCO specifications. This technique limits the maximum rate of change of a PI controller. Even though the technique guarantees not to exceed the MRCO as defined, the results could be quite disastrous. In the presence of a large disturbance, the flow rate may not be allowed to change fast enough due to the rate of change constraint, letting the tank overflow or run empty.

In conclusion, ad-hoc techniques do not directly incorporate system constraints in the design phase. The designer resorts to rule-based methods to achieve a compromise between safety and performance. In addition, as the PI algorithm has been an industrial standard for level control, it was only natural to augment the PI algorithm to achieve averaging level control. Unfortunately, the PI algorithm has no means of handling constraints and, as a result, the maximum surge capacity of the vessel cannot be fully exploited for flow smoothing.

1.1.2 Optimization-based methods

The focus of averaging level control shifted in the 1980's and it continues to follow the direction of optimization-based methods. In optimization-based methods, an optimality criterion is specified based on the desirable characteristics of the closed-loop behaviour of the system. The control action is then resolved by incorporating some optimization subroutine that minimizes a specified cost function. For averaging level control, the following optimization-based methods have been presented in the literature.

- McDonald and McAvoy were the first to incorporate MRCO and the system state constraints into controller synthesis [12]. As a result, there were two controllers proposed; a Ramp Controller (RC) and an Optimal Predictive Controller (OPC). The RC controller was based a nonlinear feedback control law that related the level in the tank to the outlet flow rate. The optimal solution sets the outlet flow rate

trajectory with the smallest MRCO subject to level constraints. As the synthesis resulted in a P control law, an integral mode or the PL scheme were augmented to eliminate any offset.

The OPC is a feedforward/feedback controller based on the predictive extension of the RC controller. At each sampling instant the flow imbalance is measured, the future optimal control policy is determined, and the first control move is implemented. It is assumed that the inlet flow is measured or inferred, and that there is negligible dead time associated with the disturbances path. The OPC controller was modified to include proportional and integral modes and thus eliminates the need for using the PL controller to eliminate level offsets. The augmentation to eliminate offset adversely affects the best achievable MRCO.

- Campo and Morari [20] recast the work by McDonald and McAvoy [12] in a discrete time, MPC framework. By using the $\mathcal{L}_\infty$ formulation, the MPC control law was computed using a linear program (LP). They showed that an analytical solution exists when input constraints are ignored. In addition, integral action was naturally introduced by defining a terminal constraint. It was also shown that, by using the plant model, the inlet flow rate could be inferred, eliminating the requirement for explicit measurement.

  Khanbaghi et al. [2] showed a successful industrial application of the above strategy. It was shown that the algorithm indeed provides excellent flow filtering while maintaining the tank within the level constraints. It was also pointed out that the inlet flow estimator as outlined in [20] is a deadbeat observer, which is extremely sensitive to process noise. As a solution to estimate the inlet flow, a Kalman filter was implemented.

- Utilization of the PI algorithm for averaging level control was reintroduced by Kelly [13]. In this formulation, the PI controller parameters were calculated via an off-line optimization. The objective of the optimization was to minimize the variance of the rate of change of the outlet flow rate for a given variance of the inlet disturbance and for the user defined tank level variance.

  Later Foley et al. [18] expanded upon [13] and presented an analytical solution for the tuning of the PI controller using a constrained Linear Quadratic (LQ) framework. This technique statistically provided a 3σ guarantee that the tank level would stay within level constraints (i.e. 99.7% of time). Sidhu et al. [17] successfully applied the algorithm to an industrial caustic dilution system.

  It should be noted that both [18] and [13] are unable to explicitly account for process constraints. Only statistical guarantees against constraint violation are promised.

- To the author's knowledge, Bonhivers et. al. [9] are the first to have considered fully interacting multiple tanks in an inventory problem. The objective of their study was to reduce the variability in the paper machine wet end and reduce fresh water consumption. A multivariable MPC controller based on Quadratic Programming (QP) was devised and implemented. The main motivation and contribution of the work was to demonstrate the application of constrained MPC for resolving the problem. In the study, no other controller design methodologies were considered.

The latest trend in resolving the averaging level control problem has been to incorporate optimization methods. MPC, particulary, allows the designer to systematically incorporate all system constraints during controller formulation. Much has been done in the realm of a single tank. The algorithm by Campo and Morari [20] provides an excellent analytical solution. However, in fully coupled multiple tank systems, very little has been done. For the proper operation of modern plants, it is essential to better understand the MIMO case.

1.2 The Industrial Process & The Lab-Scale Plant Setup

This chapter presents an industrial system that requires good flow filtering for proper operation. This industrial two-tank pressure screening system also motivated this thesis. In order to facilitate the study, a lab-scale two-tank rig was constructed that mimics the industrial system. The corresponding system model was derived based on the lab-scale system. By analyzing the process model a great deal of insight was acquired about the MIMO system.

1.2.1 The Pulp Pressure Screening System

During the mechanical pulping process, wood chips are broken down into individual fibers through the refining process. The aqueous solution, referred to as pulp, has a typical fiber consistency of 0.5 % by weight. Before pulp is sent to the paper machine, it is screened to remove any unrefined chips and debris. To increase the efficiency of the screening circuit, screens are typically arranged in a cascading fashion as illustrated in Figure 1.1. In this strategy the accepts of the primary screen are supplied to the paper machine while the rejects are passed through the secondary screen. The accepts of the secondary screen are re-introduced to the primary screen and the rejects of the secondary screen are sent for further refining. As the flow to the pressure screens must be smooth, the two tanks in Figure 1.1 serve as surge vessels.

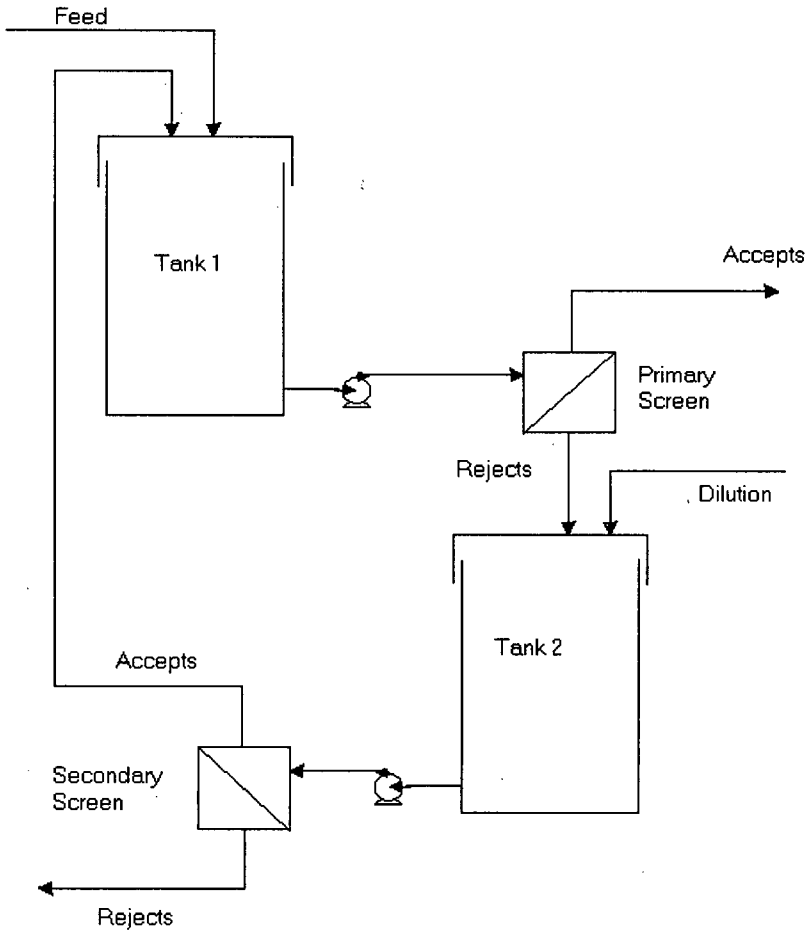

Figure 1.1: Two tank pressure screening system

Illustrated in Figure 1.2 is a typical pressure screen. As pulp enters the feed chamber it experiences enormous centrifugal forces caused by the hydrofoil. The pulp fibers of allowable size are forced through the slotted screen plate while the over-sized fibers and debris are passed to the reject outlet. The differential pressure between the feed and the accepts streams provides the driving force for the separation process [1]. Also, the reject rate is responsible for establishing the operating point of the screen. In a typical control strategy of a pressure screen, the reject flow is ratio-controlled with respect to the feed flow rate. Furthermore, the screen differential pressure is regulated by manipulating the accepts flow. Large disturbances in the feed can cause dramatic shifts in the operating point of the pressure screen. This can lead to a decrease in screening efficiency and can even plug the screen apertures. For proper operation of a pressure screen, flow disturbances must be absorbed by the surge tanks. In the industry production rate changes are common, which can be modelled as deterministic steps. If such a step disturbance was allowed to pass through the tank (possible with tight level control) and introduced to the screen, the screen

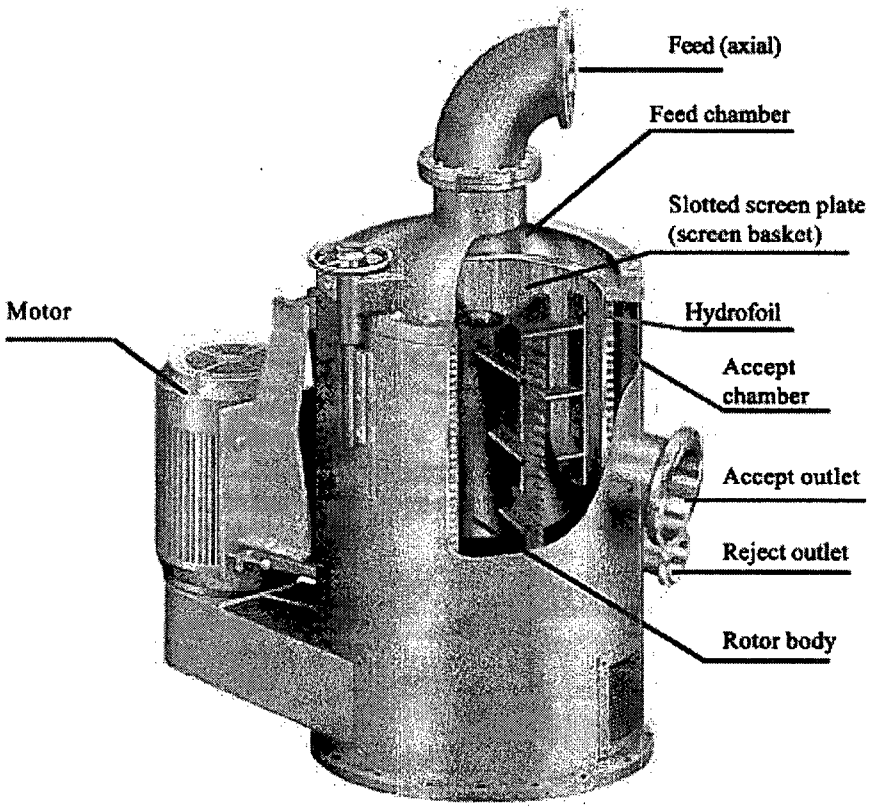

Figure 1.2: Pressure screening schematic [1]

operation can be adversely effected. Attenuating such disturbances using averaging level control would introduce the same disturbance in steps of considerably smaller magnitude over time. This also makes MRCO an excellent measure for assessing disturbance rejection capability of a averaging level controller. In the industry it is common to utilize PI controllers to independently control the level of each surge tank. As discussed earlier, a PI controller is unable to provide adequate averaging level control.

1.2.2 Laboratory Two Tank System

In order to conveniently study the pulp screening system, a laboratory-scale experimental rig was constructed. From here on the laboratory-scale experimental rig will be referred to as the "two-tank system". The fundamental assumption in constructing the two tank system was representing the pressure screens by static flow splitters. This assumption is valid as the pressure screen has relatively fast dynamics when compared to the tank level dynamics. The difference in bandwidth provides a natural decoupling between the screen dynamics and the tank level dynamics. As a result, from the level control perspective, the pressure screen is a static process. As the densities of both pulp and water are almost

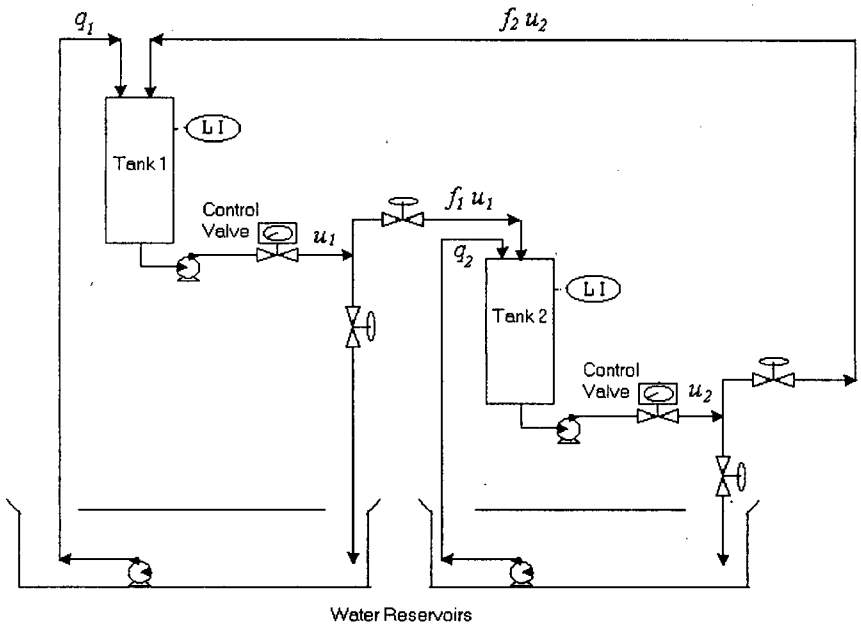

Figure 1.3: Laboratory two-tank system

	Tank 1	Tank 2
Cross-sectional area, A_c	146.0 cm^2	146.0 cm^2
Maximum tank height	35.0 cm	35.0 cm
Maximum outlet flow rate	4.0 L/min	4.0 L/min

Table 1.1: Two tank system specifications

identical, due to low pulp consistency, water was used to present pulp in the two-tank system. The two-tank system was originally an undergraduate laboratory experimental rig which was modified with the appropriate hardware and instrumentation to mimic the industrial pressure screening process. The two-tank system is illustrated in Figure 1.3 and the system specifications are given in Table 1.1.

1.2.3 Process Model and Analysis

The process model based on the two-tank system is used for analysis and controller design. The system model can be easily computed based on first principles. Using volumetric

balances around each tank, equations (1.1) and (1.2) are obtained.

$$\text{Tank 1} \qquad A_{c1}\frac{dy_1}{dt} = q_1 + f_2 \cdot u_2 - u_1 \tag{1.1}$$

$$\text{Tank 2} \qquad A_{c2}\frac{dy_2}{dt} = q_2 + f_1 \cdot u_1 - u_2 \tag{1.2}$$

where

$$\begin{aligned} y &= \text{Liquid level in the tank, } (cm) \\ A_c &= \text{Cross-sectional area of the tank, } (cm^2) \\ u &= \text{Outlet flow rate from the tank, } (L/min) \\ q &= \text{Inlet flow rate perturbation to the tank, } (L/min) \\ f &= \text{Fraction of recycle flow} \end{aligned}$$

By combining equations (1.1) and (1.2) and taking the Laplace transforms, the multivariable plant model is computed:

$$\begin{bmatrix} y_1(s) \\ y_2(s) \end{bmatrix} = \underbrace{\frac{1}{s}\begin{bmatrix} -\frac{1}{A_{c1}} & \frac{f_2}{A_{c1}} \\ \frac{f_1}{A_{c2}} & -\frac{1}{A_{c2}} \end{bmatrix}}_{G_p} \begin{bmatrix} u_1(s) \\ u_2(s) \end{bmatrix} + \underbrace{\frac{1}{s}\begin{bmatrix} \frac{1}{A_{c1}} & 0 \\ 0 & \frac{1}{A_{c2}} \end{bmatrix}}_{G_d} \begin{bmatrix} q_1(s) \\ q_2(s) \end{bmatrix} \tag{1.3}$$

where s is the Laplace transform variable. In equation (1.3), the special structure where the dynamics can be extracted from the transfer function matrix will later prove to be extremely useful. Furthermore, equation (1.3) can be discretized with sampling interval T to obtain a discrete time state-space model.

$$\begin{bmatrix} x_1(k+1) \\ x_2(k+1) \end{bmatrix} = \underbrace{\begin{bmatrix} 1 & 0 \\ 0 & 1 \end{bmatrix}}_{A} \begin{bmatrix} x_1(k) \\ x_2(k) \end{bmatrix} + \underbrace{\begin{bmatrix} -\frac{T}{A_{c1}} & \frac{Tf_2}{A_{c1}} \\ \frac{Tf_1}{A_{c2}} & -\frac{T}{A_{c2}} \end{bmatrix}}_{B} \begin{bmatrix} u_1(k) \\ u_2(k) \end{bmatrix} + \underbrace{\begin{bmatrix} \frac{T}{A_{c1}} & 0 \\ 0 & \frac{T}{A_{c2}} \end{bmatrix}}_{D_d} \begin{bmatrix} q_1(k) \\ q_2(k) \end{bmatrix}$$

$$\begin{bmatrix} y_1(k) \\ y_2(k) \end{bmatrix} = \underbrace{\begin{bmatrix} 1 & 0 \\ 0 & 1 \end{bmatrix}}_{C} \begin{bmatrix} x_1(k) \\ x_2(k) \end{bmatrix} \tag{1.4}$$

where $x(k)$ represents the system state and $x \in \Re^n, y \in \Re^p$, and $u \in \Re^m$. As the observation matrix, C, is an identity matrix the system states are in fact the tank levels. Full

state measurement is available as both tank levels can be measured.

System eigenvalues can be easily determined from the diagonal of the A matrix. As each tank represents an integrator, the system eigenvalues are on the unit circle, as expected. For a given recycle fraction, $f < 1$, additional system analysis can be carried out. The controllability of the system can be computed as, $W_c = \begin{bmatrix} B & AB \end{bmatrix}$. W_c is of rank 2, suggesting the system is controllable. Also the system is fully observable as the observability matrix, $W_o = \begin{bmatrix} C & CA \end{bmatrix}^T$, has full rank.

For a multivariable system, computing the relative gain array (RGA) can be extremely useful. The RGA clearly reveals the degree of coupling in the system. In reality, the flow fraction, f, would change depending on the operating point of the pressure screen. For various values of f, the RGA, is displayed in Table 1.2. The degree of coupling in-

Flow fraction	RGA
$f_1 = f_2 = 0.0$	$\begin{bmatrix} 1 & 0 \\ 0 & 1 \end{bmatrix}$
$f_1 = f_2 = 0.4$	$\begin{bmatrix} 1.19 & -0.19 \\ -0.19 & 1.19 \end{bmatrix}$
$f_1 = f_2 = 0.7$	$\begin{bmatrix} 1.96 & -0.96 \\ -.96 & 1.96 \end{bmatrix}$
$f_1 = f_2 = 1.0$	∞

Table 1.2: RGA analysis

creases dramatically as the amount of recycle flow to each tank is increased. This can be seen clearly in Table 1.2 as the off-diagonal elements become large as recycle fraction is increased. When $f_1 = f_2 = 0$ the system is naturally decoupled, and the two tanks will respond independent of one another. In this case, a SISO level controller on each tank is sufficient. As the degree of coupling is increased, the interactions in the system are apparent. In the extreme, when $f_1 = f_2 = 1$, the controllability matrix loses its rank and the system is no longer controllable. Essentially, the entire control authority is utilized in mitigating the recycle load and any additional disturbance in the system cannot be removed. This can clearly render the system unstable.

Another closely related factor that needs to be examined is the magnitude of the load disturbance. If the disturbance path gain becomes greater than the loop gain, then the system is also not controllable. The disturbance path gain can increase in cases when a disturbance of greater magnitude than the maximum allowable control action is introduced. When there is a fixed control authority, there is an upper bound on the maximum inlet disturbance magnitude. In the two-tank system when the maximum control authority is $2L/min$ and assuming $q_2 = 0$, then equation (1.5) can be used to determine the

maximum attenuable tank 1 load disturbance.

$$q_1^{max} = (1 - f_1 f_2) u_1^{max} \tag{1.5}$$

Furthermore, as the degree of the recycle fraction increases, the control authority available for disturbance rejection decreases, as shown in Table 1.3. This, in fact, is a process

Flow fraction	$q_1^{max}\,(L/min)$
$f_1 = f_2 = 0.0$	2.00
$f_1 = f_2 = 0.4$	1.68
$f_1 = f_2 = 0.7$	1.02
$f_1 = f_2 = 1.0$	0.00

Table 1.3: Maximum attenuable tank 1 load disturbance under fixed control authority

design problem which must be considered at the time of tank, pump and valve selection. Analysis of the system model indicates that some form of multivariable control is required to account for system interactions.

RGA analysis has indicated that as the recycle flow fraction increases, the coupling in the system becomes stronger. From this analysis, the matter of selecting an appropriate control strategy arises. Namely, for a MIMO averaging level control problem, which is required: a decentralized controller, a decoupling controller, or a full multivariable controller? It was shown in the literature review that MPC based techniques are well suited for processes with state and actuator constraints. Then the question that needs to be answered is which MPC cost function should be minimized, the quadratic norm ($\mathcal{L}_2$), or the infinity-norm ($\mathcal{L}_\infty$)?

Answering these questions is the objective of this thesis. Theory and design of various algorithms are considered in Chapter 2. Analysis of each algorithm and its possible suitability for averaging level control is discussed. Simulation results for both single and multiple tank systems are presented in Chapter 3. The shortcomings of some control algorithms are demonstrated. In order to mitigate a problem with the ($\mathcal{L}_\infty$) norm MPC formulation with terminal constraints, a variation of the formulation is presented and compared in Chapter 4. After presenting various algorithms and conducting a comparative simulation study, some algorithms are selected for verification in a real-time application. Chapter 5 presents the real time application on a lab-scale two-tank system. Finally, Chapter 6 presents conclusions from the work presented in this thesis and makes recommendations for future work.

Chapter 2

Theory and Design of Multivariable Averaging Level Controllers

As discussed in section 1.1, there are many methodologies for achieving averaging level control in the SISO framework. But very little has been discussed in the literature about fully interacting multiple tank systems. An attempt is made in this chapter to investigate some algorithms which may be suitable for MIMO averaging level control. This chapter first presents the most basic form of multivariable control, which is decentralized control. The discussion is followed by presenting the decoupling control design, as this represents the next level of complexity in multivariable controller design. Finally full multivariable control techniques are considered which optimize specified objective functions using appropriate optimization techniques. First the MPC formulation based on $\mathcal{L}_2$ norm is considered and followed by the MPC formulation using $\mathcal{L}_\infty$ norm with terminal constraints.

2.1 Decentralized CMA

Decentralized control can be considered the most rudimentary form of multivariable control. In this formulation no consideration is given to process interactions. The interactions are ignored and diagonal controller design is performed. In some situations, where process cross coupling is weak, decentralized control can achieve almost the equivalent performance of a full interacting multivariable design [7]. Under such circumstances, proven SISO controller design techniques can be exploited. Furthermore, decentralized control is simpler to implement and understand. The most important aspect of decentralized control is the input/output pairing. As originally suggested in [3], the RGA can also be used for input/output pairing. It is suggested that the pairing should be performed between variables which have a RGA element close to +1. From the RGA analysis in section 1.2.3 it can be seen that for the two-tank system, y_1 should be controlled using u_1 and y_2 using u_2. In the case of the two-tank system the pairing is also obvious and intuitive.

As discussed in the literature review, the algorithm proposed by Campo and Morari [20] is extremely powerful. It explicitly minimizes the MRCO while maintaining the tank level within the specified level constraints. The single tank model can be obtained using equation (1.1) by setting $f_2 = 0$ and discretizing using sampling time (T) to obtained;

$$y(k+1) = y(k) + \frac{T}{A_c}q(k) - \frac{T}{A_c}u(k) \tag{2.1}$$

As outlined in [20] the problem can be formulated as:

$$\begin{aligned} &\min \parallel \nabla U \parallel^{\infty} \\ &\text{subject to} \\ &y_{min} \leq y(k) \leq y_{max} \\ &u_{min} \leq u(k) \leq u_{max} \\ &y(k+N_u) = r \end{aligned} \tag{2.2}$$

the optimization is performed over $\Re^{N_u}$, where N_u and r are control prediction horizon and setpoint, respectively. According to the formulation, in defining a terminal constraint, it is required that at the end of the prediction horizon the level must be at its setpoint. The above cost function formulation leads to a LP optimization that must be executed at each sample time. However, as shown in [20], when flow rate constraints are ignored an analytical solution exists. The analytical algorithm can be summarized by performing the following calculations at each iteration [2]:

- Evaluate the flow imbalance

$$\Omega = \frac{A_c}{T}[y(k) - y(k-1)] \tag{2.3}$$

  Using the plant model the load disturbance can be estimated and the requirement for inlet flow rate measurement is eliminated.

- Evaluate $k^{\star}$

$$k^{\star} = \mathrm{N}\left\{\frac{2A_c[y_{lim} - y(k)]}{T\Omega}\right\} \tag{2.4}$$

  where $\mathrm{N}\{i\}$ is the smallest integer $\geq i$. The time it takes to reach the level constraint from the current level is computed using the tank model and the estimated flow imbalance.

- Evaluate

$$\nabla u^0 = \frac{2\Omega}{N_u + 1} + \frac{2A_c[y(k) - r]}{TN_u(N_u + 1)} \tag{2.5}$$

$$\nabla u^\star = \frac{2\Omega(i)}{k^\star + 1} - \frac{2A_c[y_{lim} - y(k)]}{Tk^\star(k^\star + 1)} \tag{2.6}$$

where

$$y_{lim} = \text{ Tank level constraints, } y_{max} \text{ or } y_{min}$$
$$\nabla = \text{Difference operator: } \nabla u(k) = u(k) - u(k-1)$$

The controller produces two control action, ∇u^0 and $\nabla u^\star$. In order to ensure that level constraints are satisfied the nonlinear $\nabla u^\star$ is computed and ∇u^0 ensures zero steady state error. Furthermore, y_{lim} is chosen to be y_{max} if the flow imbalance is positive and y_{min} if the flow imbalance is negative.

- Select the rate of change, ∇u, to be ∇u^0 or $\nabla u^\star$ such that it has the greatest magnitude, and implement the next flow rate change as $u(k) = u(k-1) + \nabla u$

  The computed control action is integrated and applied to the plant. The control action of the maximum absolute magnitude is implemented as when level constraints are active then $\nabla u^\star > \nabla u^0$ and ensures constraint satisfaction and when level constraints are not active then $\nabla u^0 > \nabla u^\star$ and steers the level to its setpoint.

Using N_u as the only tuning knob, the closed-loop response can be specified as tight (small N_u) or averaging level control (large N_u). In the study by [20], it is also demonstrated that, for a given load step disturbance no other controller will have smaller MRCO while satisfying level constraints, provided that N_u satisfies

$$N_u \geq N_u^\dagger = \frac{1}{2 \mid \nabla u^\star \mid}\left\{2 \mid \Omega \mid + \left[(|\nabla u^\star| - 2|\Omega|)^2 + \frac{8A_c}{T}|[y(t) - r]\nabla u^\star|\right]^{\frac{1}{2}}\right\} - \frac{1}{2} \tag{2.7}$$

where $N_u^\dagger$ is the critical prediction horizon. The algorithm is able to handle level constraints by design but lacks the ability to handle flow rate or input constraints. It is stated in [20] that numerical optimization is required in order to optimally handle flow rate constraints. In fact, it can be shown that input constraints for the SISO case can be handled by using the following simple anti-windup strategy, computed as:

$$sat\{u(k)\} = \begin{cases} u_{max} & u(k) > u_{max} \\ u(k) & u_{min} < u(k) < u_{max} \\ u_{min} & u(k) < u_{min} \end{cases} \tag{2.8}$$

From here on Campo & Morari's algorithm augmented with the anti-windup circuit will be referred to as CMA. This leads to the following theorem:

Theorem 2.1. *Provided $N_u \geq N_u^{\dagger}$, equation (2.7), is satisfied then CMA can handle level and flow rate constraint while providing a MRCO optimal solution.*

Proof. Let $u(k) \in \mathcal{U}$, where $\mathcal{U}$ is a closed set of all admissible control actions. For any controller to stabilize an unstable system in the face of a load disturbance, q, it is required that $q \in \mathcal{U}$ also holds. In [12], by definition $\|\nabla u_{max}\|_\infty \leq q$ is always true. Hence clipping the control action has no effect on the MRCO optimality of CMA. □

The aforementioned proof shows that no numerical optimization is required to satisfy both level and flow rate constraints.

In further analyzing the CMA algorithm, it is interesting to note that equation (2.5) constitutes the linear part of the CMA algorithm. This is the minimum change in flow rate required to bring the level to setpoint, such that the terminal constraint is enforced (refer to equation (2.2)). Whereas equation (2.6) constitutes the nonlinear part of the algorithm which is the smallest rate of change to the flow rate required to prevent level constraint violation. After simple manipulations, the linear portion of the CMA algorithm can be shown to be identical to a PI controller. A general equation for the discrete time PI controller is shown in equation (2.9), where z^{-1} is the backward shift operator.

$$G_{PI}(z^{-1}) = \frac{K_c[(1 + T/T_r) - z^{-1}]}{\nabla} \tag{2.9}$$

Equation (2.9) can be shown to be equal to equation (2.5) if the PI parameters are selected as follows.

$$K_c = \frac{-2A_c}{T(N_u + 1)}, \qquad \frac{T}{T_r} = \frac{1}{N_u}$$

This equivalence also provides a very convenient method of tuning a PI controller for level control. It was pointed out in [21] that the optimal damping factor for an averaging level controller is $\frac{\sqrt{2}}{2}$. In Figure 2.1, the system closed-loop poles are illustrated as N_u varies. It is interesting to note that the closed loop poles are situated along the $\frac{\sqrt{2}}{2}$ damping contour. Also it can be seen that by selecting $N_u = 1$, a deadbeat response is realized as

both of the closed-loop poles are placed at the origin of the unit z-plane. As $N_u \longrightarrow \infty$ the closed-loop poles traverse through the complex plane along the $\frac{\sqrt{2}}{2}$ damping contour towards unity. At unity the closed-loop poles have approached the open loop pole and the system is essentially in open-loop.

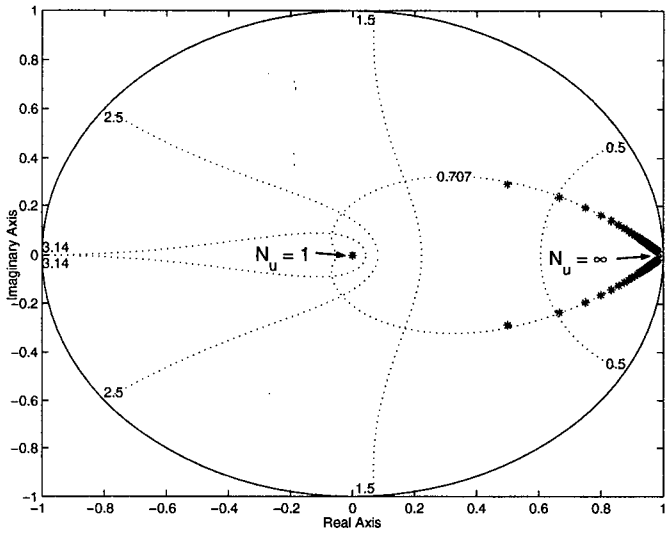

Figure 2.1: Closed-loop poles with varying N_u

The CMA algorithm possesses characteristics which are essential for averaging level control. In the decentralized framework, the CMA controller can be used to control each tank. For the two-tank system the decentralized controller structure is as follows

$$G_c = \begin{bmatrix} CMA_1 & 0 \\ 0 & CMA_2 \end{bmatrix}$$

and the control configuration is illustrated in Figure 2.2. Similarly the PI algorithm

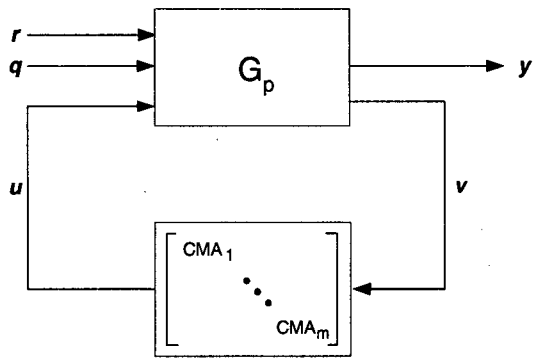

Figure 2.2: Decentralized CMA control configuration

can be introduced along the main diagonal to obtain a decentralized PI controller. In this

framework, no attempt is made to account for the system interactions as the off-diagonal elements of the controller are zero. Each controller on the diagonal can be individually tuned for the desired response in the corresponding tank. This framework may not lead to optimal controller performance, but the controller structure is simple and it provides an excellent starting point for multivariable controller design.

2.2 Decoupled CMA

In the next level of multivariable control, an attempt is made to account for system interactions. Decoupling is a technique which attempts to reduce or eliminate closed-loop interactions [5]. The objective is to transform the system mathematically to remove any interactions. In practice, it is rare that complete decoupling is possible across all frequencies. Various methods for decoupling exist depending on the requirements, ranging from steady state decoupling to decoupling using state feedback [11].

As discussed in section 1.2.3, the multiple tank system has a very unique system model. The multiple tank model can be separated into scalar dynamics multiplied by a constant matrix.

$$\begin{bmatrix} y_1(s) \\ \\ y_2(s) \end{bmatrix} = \frac{1}{s} \underbrace{\begin{bmatrix} -\frac{1}{A_{c1}} & \frac{f_2}{A_{c1}} \\ \\ \frac{f_1}{A_{c2}} & -\frac{1}{A_{c2}} \end{bmatrix}}_{\widetilde{A}} \begin{bmatrix} u_1(s) \\ \\ u_2(s) \end{bmatrix} \tag{2.10}$$

Equation (2.10) has the form $G(s) = k(s)\widetilde{A}$ where $k(s) = \frac{1}{s}$ represents the scalar dynamics and $\widetilde{A}$ is the constant matrix. For such models, dynamic decoupling across all frequencies is possible using only a scalar transformation [14].

Lemma 2.1. *The multiple tank system can be dynamically decoupled using the constant decoupling matrix defined as* $W = \widetilde{A}^{-1}\widetilde{A}_{diag}$. *This transformation preserves the original plant along the diagonal elements.*

Proof. The proof is straightforward as shown below.

$$W = \widetilde{A}^{-1}\widetilde{A}_{diag}$$

$$G_p^{decoupled} = \frac{1}{s}\widetilde{A}W = \frac{1}{s}\begin{bmatrix} -\frac{1}{A_{c1}} & 0 \\ \\ 0 & -\frac{1}{A_{c2}} \end{bmatrix}$$

□

Lemma 2.2. *CMA is guaranteed to maintain the tank level within its constraints for a step load disturbance.*

Proof. As shown in [20]. □

Theorem 2.2. *For a multiple tank system which is dynamically decoupled by preserving the diagonal elements, and assuming no input constraints are encountered, then the Decentralized CMA controller is guaranteed to satisfy tank level constraints.*

Proof. The proof is simple by combining Lemma 2.1 and Lemma 2.2.

□

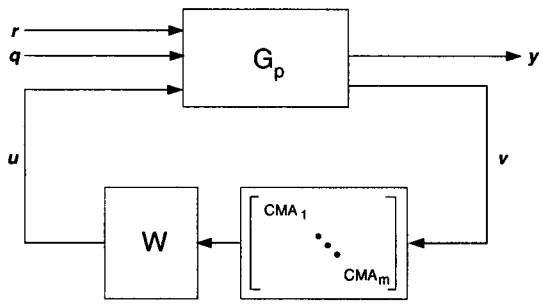

Figure 2.3: Decoupled CMA control configuration

Using a constant decoupling matrix to decouple the multivariable system across all frequencies is extremely useful. By combining the decoupling matrix and using decentralized control, tank level constraints can be successfully handled. The Decoupled CMA control configuration is illustrated in Figure 2.3. In the case of input constraints, however, the solution is not trivial. During actuator saturation only partial decoupling can be accomplished [7]. Under partial decoupling Theorem 2.2 is no longer satisfied and there is no guarantee in handling level constraints. In order to optimally handle all system constraints, constrained optimization is usually required [15], which is the focus of the remainder of this chapter.

2.3 $\mathcal{L}_2$ MPC using QP: MPCQP

Model based predictive control is the only control methodology that allows the designer to account for all process constraints in a systematic manner [15]. In this section, the state space formulation of MPC is presented. By working in the state space framework, no generality of MPC is lost as polynomial-based techniques such as DMC and GPC can all be realized equivalently [8].

In the standard state-space formulation of the constrained MPC control law, the following $\mathcal{L}_2$ norm cost function is minimized:

$$V_{\nabla u}(k) = \sum_{i=N_1}^{N_2} \| y(k+i) - r(k+i) \|^2_{Q(i)} + \sum_{i=0}^{N_u-1} \| \nabla u(k+i) \|^2_{R(i)}$$

$$\text{subject to:} \tag{2.11}$$

$$y_{min} \leq y(k) \leq y_{max}$$

$$u_{min} \leq u(k) \leq u_{max}$$

where N_1, N_2 are the minimum prediction horizon and the maximum prediction horizon, respectively. Also, $Q(i)$ is the output weight matrix and $R(i)$ is the input weight matrix. As a note, Q and R carry the same interpretation as in LQ controller design. As it can be seen in (2.11), the minimization is performed with respect to ∇u rather than u. It is quite convenient to optimize with respect to ∇u as the effect of the mean value is removed.

Consider the linear time-invariant (LTI) state-space model:

$$\begin{aligned} x(k+1) &= Ax(k) + Bu(k) \\ y(k) &= Cx(k) \end{aligned} \tag{2.12}$$

In equation (2.12), $x(k) \in \Re^n$ is the system state vector, $u(k) \in \Re^m$ is the input control vector and $y(k) \in \Re^p$ is the system output vector. In order to introduce ∇ in the cost function the state-space model is modified. The augmented state-space model can be presented by the state vector

$$\xi(k) = \begin{bmatrix} \nabla x(k) \\ y(k) \end{bmatrix} \tag{2.13}$$

where $\nabla x(k) = x(k) - x(k-1)$. From equation (2.12),

$$x(k) = Ax(k-1) + Bu(k-1) \tag{2.14}$$

Now subtracting equation (2.14) from (2.12) gives

$$\nabla x(k+1) = A\nabla x(k) + B\nabla u(k) \tag{2.15}$$

Also from equation (2.12), the one-step-ahead output vector is:

$$\begin{aligned} y(k+1) &= Cx(k+1) \\ &= C[\nabla x(k+1) + x(k)] \\ &= C[A\nabla x(k) + B\nabla u(k)] + y(k) \end{aligned} \tag{2.16}$$

Now the state-space augmented system is defined as,

$$\begin{bmatrix} \nabla x(k+1) \\ y(k+1) \end{bmatrix} = \underbrace{\begin{bmatrix} A & 0 \\ CA & I \end{bmatrix}}_{\hat{A}} \begin{bmatrix} \nabla x(k) \\ y(k) \end{bmatrix} + \underbrace{\begin{bmatrix} B \\ CB \end{bmatrix}}_{\hat{B}} \nabla u(k)$$

$$\begin{bmatrix} y(k) \end{bmatrix} = \underbrace{\begin{bmatrix} 0 & I \end{bmatrix}}_{\hat{C}} \begin{bmatrix} \nabla x(k) \\ y(k) \end{bmatrix} \tag{2.17}$$

Assuming $\nabla u(k+j) = 0$ for $N_u < j \leq N_2$ or the changes in the control action are set to zero past the control horizon, and using the above augmented state-space model the state trajectory can be predicted as:

$$\Xi(k) = \begin{bmatrix} \xi(k+1) \\ \cdot \\ \cdot \\ \cdot \\ \xi(k+N_2) \end{bmatrix} = \mathcal{F}\xi(k) + \mathcal{G}\nabla U(k) \tag{2.18}$$

where $\nabla U(k) = [\nabla u(k), \cdots, \nabla u(k+N_u-1)]$ and the matrices $\mathcal{F}$ and $\mathcal{G}$ are defined as:

$$\mathcal{F}(k) = \begin{bmatrix} \hat{A} \\ \hat{A}^2 \\ \cdots \\ \prod_{j=N_2-1}^{0} \hat{A}(j) \end{bmatrix}$$

$$\mathcal{G}(k) = \begin{bmatrix} \hat{B} & 0 & \cdots & 0 \\ \hat{A}\hat{B} & \hat{B} & \cdots & 0 \\ \vdots & \vdots & \ddots & \vdots \\ [\prod_{j=N_u-1}^{1} \hat{A}(j)]\hat{B} & [\prod_{j=N_u-1}^{2} \hat{A}(j)]\hat{B} & \cdots & \hat{B} \\ \vdots & \vdots & \ddots & \vdots \\ [\prod_{j=N_2-1}^{1} \hat{A}(j)]\hat{B} & [\prod_{j=N_2-1}^{2} \hat{A}(j)]\hat{B} & \cdots & [\prod_{j=N_2-1}^{N_u} \hat{A}(j)]\hat{B} \end{bmatrix}$$

As previously stated, the cost function being minimized is

$$V_{\nabla u}(k) = \sum_{j=N_1}^{N_2} \| C\xi(k+j) - r(k+j) \|^2_{Q(j)} + \sum_{j=0}^{N_u-1} \| \nabla u(k+j) \|^2_{R(j)} \tag{2.19}$$

that can be expanded and rewritten as,

$$\begin{aligned} V_{\nabla U}(k) = {} & \nabla U(k)^T [\mathcal{G}^T \mathcal{C}^T \mathcal{Q} \mathcal{C} \mathcal{G} + \mathcal{R}] \nabla U(k) \\ & + 2[[\mathcal{F}\xi(k)]^T \mathcal{C}^T - \bar{r}(k)^T] \mathcal{Q} \mathcal{C} \mathcal{G} \nabla U(k) + \mathcal{X}(k) \end{aligned} \tag{2.20}$$

where

$$\mathcal{Q} = \begin{bmatrix} Q(1) & & \\ & \ddots & \\ & & Q(N_2) \end{bmatrix}$$

$$\mathcal{R} = \begin{bmatrix} R(1) & & \\ & \ddots & \\ & & R(N_u) \end{bmatrix}$$

$$\mathcal{C} = \begin{bmatrix} \hat{C}(1) & & \\ & \ddots & \\ & & \hat{C}(N_2) \end{bmatrix}$$

$$\bar{r}(k) = [r(k+1)^T, \cdots, r(k+N_2)^T]^T$$

The $\mathcal{X}(k)$ term can be dropped from the cost function as it has no effect on the optimal solution. To further reduce equation (2.20), let $\mathcal{A} = \mathcal{G}^T\mathcal{C}^T\mathcal{Q}\mathcal{C}\mathcal{G} + \mathcal{R}$ and let $\mathcal{B} = 2[[\mathcal{F}\xi(k)]^T\mathcal{C}^T - \bar{r}(k)^T]\mathcal{Q}\mathcal{C}\mathcal{G}$. Then by taking the gradient of $V(k)$ and setting it equal to zero the unconstrained MPC solution is computed as

$$\nabla U(k) = -\frac{1}{2}\mathcal{A}^{-1}\mathcal{B}^T \tag{2.21}$$

The unconstrained MPC control law is linear and unable to handle any system constraints. Fortunately it is quite straightforward and simple to define system constraints (i.e. state, input, slew rate constraints). This is actually one of the most attractive features of MPC. In this formulation, constraints are defined on the input magnitude, the input slew rate and on system states. Other constraints such as the terminal constraint set, over-shoot constraints and undershoot constraints can also be easily defined [6].

- Input Magnitude Constraints: As in all practical applications, actuators have finite authority. Therefore, constraints must be defined on the magnitude of the control action to prevent integrator windup. The constraints on the input magnitude are

defined as

$$m_{min}(k) \leq u(k) \leq m_{max}(k)$$

$$\mathbb{M} \cdot m_{min}(k) \leq U(k) \leq \mathbb{M} \cdot m_{max}(k) \tag{2.22}$$

$$\alpha \leq U(k) \leq \beta$$

where

$$\mathbb{M} = \begin{bmatrix} I_m \\ \vdots \\ I_m \end{bmatrix}$$

and $\mathbb{M} \in \Re^{mNu,m}$. As the optimization will be performed with respect to ∇U rather than U, then the constraints must also be defined in terms of ∇U. This can be achieved by using the following modification:

$$u(k+i-1) = u(k-1) + \sum_{j=0}^{i-1} \nabla u(k+j)$$

in matrix notation

$$U(k) = \Lambda \nabla U(k) + \mathcal{I} u(k-1)$$

$$\Lambda = \begin{bmatrix} I_m & 0 & \cdots & 0 \\ I_m & I_m & \cdots & 0 \\ \vdots & \vdots & \ddots & \vdots \\ I_m & I_m & I_m & I_m \end{bmatrix} \tag{2.23}$$

$$\mathcal{I} = [I_m, \cdots, I_m]^T$$

Now with the above modification, the magnitude constraints on input can be expressed in terms of ∇U.

- Input Rate Constraints: It is also quite realistic that actuators have limited rates of

change. Rate constraints on the input can be represented as

$$l_{min}(k) \leq \nabla u(k) \leq l_{max}(k)$$

$$\mathbb{M} \cdot m_{min}(k) \leq \nabla U(k) \leq \mathbb{M} \cdot m_{max}(k) \tag{2.24}$$

$$\psi \leq \nabla U(k) \leq \omega$$

- State/Output Constraints: In the case of averaging level control, the state or output constraints are the most important constraints. State constraints can also be easily defined within the MPC framework as

$$n_{min}(k) \leq \xi(k) \leq n_{max}(k)$$

$$\mathbb{N} \cdot n_{min}(k) \leq \Xi(k) \leq \mathbb{N} \cdot n_{max}(k) \tag{2.25}$$

$$\gamma \leq \Xi(k) \leq \delta$$

where

$$\mathbb{N} = \begin{bmatrix} I_{n+p} \\ \vdots \\ I_{n+p} \end{bmatrix}$$

and $\mathbb{N} \in \Re^{N_2(n+p),(n+p)}$. The state constraints also need to be expressed in terms of ∇U. This can be accomplished by mapping the state constraints as constraints on ∇U by using the state prediction equation (2.18).

The constrained MPC formulation can now be stated as follows:

$$\min \nabla U^T \mathcal{A} \nabla U + \mathcal{B} \nabla U \tag{2.26}$$

subject to the linear inequality constraints:

$$\mathcal{D} \nabla U \leq \mathcal{E}$$

where

$$\mathcal{D} = \begin{bmatrix} \Lambda \\ -\Lambda \\ I \\ -I \\ \mathcal{G} \\ -\mathcal{G} \end{bmatrix} \qquad \mathcal{E} = \begin{bmatrix} \beta - \mathcal{I}u(k-1) \\ -\alpha + \mathcal{I}u(k-1) \\ \omega \\ -\psi \\ \delta - \mathcal{F}\xi(k) \\ -\gamma + \mathcal{F}\xi(k) \end{bmatrix}$$

The optimal solution to the problem as formulated is obtained via QP optimization. The first term of the calculated control sequence is passed through an integrator and then applied to the plant. The optimal control is computed at the next sampling time and the control action continues to be applied in a receding horizon fashion.

The choice of MPCQP as a candidate algorithm for averaging level control is well justified. The MPCQP algorithm can naturally incorporate system constraints and, via QP optimization, can provide $\mathcal{L}_2$ optimal control actions. The algorithm is also easy to tune as the controller weights Q and R, along with the horizons, may be adjusted to achieve the desired closed-loop behavior. Provided that input and output have been appropriately scaled, then by setting R to be larger than Q the control actions are heavily penalized providing flow smoothing. The algorithm can be significantly detuned as it is capable of making more aggressive corrective actions if system constraints are approached.

2.4 $\mathcal{L}_\infty$ MPC with Terminal Constraints using LP: CMN

An alternative to employing the QP algorithm is to reformulate the MPC cost function and cast the problem as a LP optimization. Keeping with the spirit of Campo & Morari [20], the constrained MIMO MPC using LP optimization is formulated by minimizing the $\mathcal{L}_\infty$ norm, similar to equation (2.2). From here on this algorithm will be referred to as CMN. The requirement of averaging level control is to minimize the maximum rate of change, so it is only natural to minimize the largest change in the control action or minimize its $\mathcal{L}_\infty$ norm. Minimization with respect to the $\mathcal{L}_1$ norm also leads to LP optimization. But in the $\mathcal{L}_1$ formulation, large deviations in control action may be allowed. The formulation in [20], which was developed for a truncated impulse response model, is now extended to the general MIMO state-space framework.

For the $\mathcal{L}_\infty$ MPC formulation the following cost function is defined:

$$\begin{aligned} &\min \sum_{i=1}^{m} \| \nabla U_i(k) \|_R^\infty \\ &\text{subject to:} \\ &\qquad y_{min} \leq y \leq y_{max} \\ &\qquad u_{min} \leq u \leq u_{max} \\ &\qquad y(k+N_u) = r(k) \end{aligned} \tag{2.27}$$

In the above formulation $N_1 = 1$, and $N_2 = N_u$ and thus the minimization is over $\Re^{mNu}$. The cost function can be defined as a Chebyshev approximation problem by defining

$$\mu^\star = \sum_{i=1}^{m} \| \nabla U \|_R^\infty \tag{2.28}$$

Then any μ that satisfies

$$\begin{aligned} -\mathbf{1}_{N_u}\, \mu &\leq -\mathcal{H}\mathcal{R}\nabla U \\ -\mathbf{1}_{N_u}\, \mu &\leq \mathcal{H}\mathcal{R}\nabla U \end{aligned} \tag{2.29}$$

is an upper bound on $\mu^\star$. In equation (2.29), $\mathcal{H}$ is defined as

$$\mathcal{H} = \begin{bmatrix} \mathbf{1}_m^T & & \\ & \ddots & \\ & & \mathbf{1}_m^T \end{bmatrix}$$

and where $\mathbf{1}$ is a column vector of ones with the appropriate dimension. The constraints can be defined as in equations (2.22), (2.24) and (2.25) for input magnitude, input slew rate and states, respectively. Now the problem can be formulated as:

$$\min_{\mu \nabla U} \mu$$

subject to

$$\begin{aligned}
\mathbf{0} &\geq -\mathbf{1}_{N_u}\,\mu + \mathcal{H}\mathcal{R}\nabla U \\
\mathbf{0} &\geq -\mathbf{1}_{N_u}\,\mu - \mathcal{H}\mathcal{R}\nabla U \\
\delta &\geq \mathcal{F}\xi(k) + \mathcal{G}\nabla U \\
-\gamma &\geq -\mathcal{F}\xi(k) - \mathcal{G}\nabla U \\
\mathbf{0} &\geq -\nabla U + \psi \\
\omega &\geq \nabla U \\
\beta &\geq \Lambda\nabla U(k) + \mathcal{I}u(k-1) \\
-\alpha &\geq -\Lambda\nabla U(k) - \mathcal{I}u(k-1) \\
\mathcal{K}\bar{r}(k) &= \mathcal{K}\mathcal{C}\mathcal{F}\xi(k) + \mathcal{K}\mathcal{C}\mathcal{G}\nabla U \\
-\mathcal{K}\bar{r}(k) &= -\mathcal{K}\mathcal{C}\mathcal{F}\xi(k) - \mathcal{K}\mathcal{C}\mathcal{G}\nabla U
\end{aligned}$$

where

$$\mathcal{K} = \begin{bmatrix} \mathbf{0}_{p,p} & & \\ & \ddots & \\ & & \mathbf{I}_p \end{bmatrix}$$

is defined to induce terminal constraints with $\mathbf{0}$ being a matrix of zeros of appropriate dimensions. According to the above formulation it is required that the process output be at the specified setpoint at the end of the prediction horizon.

Furthermore, by defining $\overline{\nabla U} = \nabla U - \psi$ the above formulation can be cast into the standard LP framework.

$$\min_{x} \mathtt{c}^T\mathtt{x}$$

subject to:

$$\begin{aligned}
\mathtt{A}_1\mathtt{x} &\leq \mathtt{b}_1 \\
\mathtt{A}_2\mathtt{x} &= \mathtt{b}_2 \\
\mathtt{x} &\geq \mathbf{0}
\end{aligned} \tag{2.30}$$

where

$$\mathtt{c} = \begin{bmatrix} 1 \\ \mathbf{0} \end{bmatrix} \qquad \mathtt{x} = \begin{bmatrix} \mu \\ \overline{\nabla U} \end{bmatrix}$$

$$\mathtt{A}_1 = \begin{bmatrix} -1 & \mathcal{HR} \\ -1 & -\mathcal{HR} \\ \mathbf{0} & \mathcal{G} \\ \mathbf{0} & \mathcal{G} \\ \mathbf{0} & \mathbf{I} \\ \mathbf{0} & \Lambda \\ \mathbf{0} & -\Lambda \end{bmatrix} \qquad \mathtt{b}_1 = \begin{bmatrix} -\mathcal{HR}\psi \\ \mathcal{HR}\psi \\ \delta - \mathcal{F}\xi(k) - \mathcal{G}\psi \\ -\gamma - \mathcal{F}\xi(k) - \mathcal{G}\psi \\ \omega - \psi \\ \beta - \Lambda\psi - \mathcal{I}u(k-1) \\ \alpha = \Lambda\psi = \mathcal{I}u(k-1) \end{bmatrix}$$

$$\mathtt{A}_2 = \begin{bmatrix} \mathbf{0} & \mathcal{KCG} \\ \mathbf{0} & -\mathcal{KCG} \end{bmatrix} \qquad \mathtt{b}_2 = \begin{bmatrix} \mathcal{K}\overline{r}(k) - \mathcal{KCF}\xi(k) \\ -\mathcal{K}\overline{r}(k) + \mathcal{KCF}\xi(k) \end{bmatrix}$$

For averaging level control, CMN has the same characteristics as MPCQP such that constraints can be easily incorporated into the design phase. Furthermore, the CMN algorithm explicitly minimizes the MRCO, which is the fundamental objective of averaging level control.

Various MIMO controller design techniques have been presented in this chapter. Now it is natural to compare and contrast the various algorithms and determine the best strategy. This is the focus of the next chapter.

Chapter 3

Controller Comparison: Simulation Results

In the previous chapter, several algorithms for averaging level control were developed. The objective of this chapter is to systematically analyze these algorithms and establish their suitability for averaging level control.

This chapter first establishes the differences between tight and averaging level control, and shows why tight level control is not desired when flow smoothing is the primary objective. Next, a comparative study of the various algorithms for a single tank system is presented, followed by a comparative study for the two-tank system. The effect of various cost functions in MPC formulation is also discussed.

3.1 Tight versus Averaging Level Control

Averaging level control provides flow smoothing by transferring flow variability to the tank level. It is common in industry to utilize a PI controller that is tuned for tight level control. The tightly tuned controller transmits flow disturbances through the tank, defeating the purpose of a surge vessel.

A single tank from the two-tank system is discussed in this section (see section 1.2.2). The tank level is controlled using a PI controller which manipulates the outlet flow rate and a step disturbance is introduced at the inlet. Table 3.1 contains the simulation parameters and the sampling time, T, is 10 seconds. For ease of comparison, the nominal

Cross-sectional area, A_c	146.0 cm^2
Nominal level, r	0.0 cm
Inlet disturbance, q	1.2 L/min

Table 3.1: Simulation parameters

setpoint and nominal flow rates are subtracted from the actual values in order to center the level and the flow rate around zero. The differences between tight and averaging level control for a inlet flow disturbances of 1.2 L/min are illustrated in Figure 3.1. It can be seen that the tightly tuned PI controller deploys aggressive control action for quick disturbance rejection; this invariably results in a large MRCO. On the other hand, the PI controller tuned to provide averaging level control allows the tank level to deviate significantly from setpoint and absorbs the flow disturbance. The MRCO for tight level control

and for averaging level control in this example are 3.6 $L/min/min$ and 0.11 $L/min/min$, respectively. In order to achieve averaging level control, manipulations in the flow rate

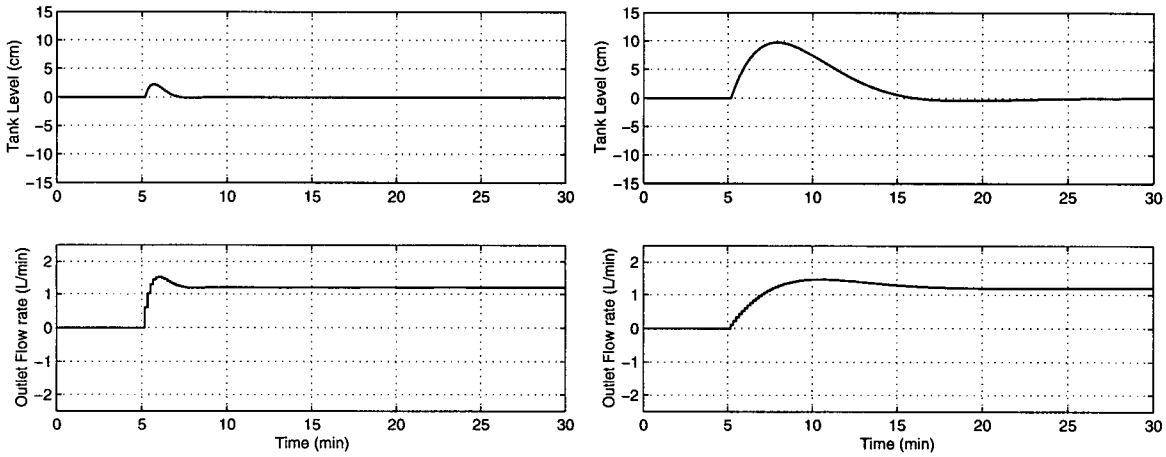

(a) Tight level control (b) Averaging level control

Figure 3.1: Tight level control vs. Averaging level control

must be minimized. In the next section, a detailed comparison of various averaging level control algorithms for a single tank are discussed.

3.2 Single Tank Averaging Level Control

Initially studying the problem in a single dimension using a SISO tank system can be extremely instructive. This can provide excellent insights into the behaviour of various control algorithms and pave the way for analysis of the MIMO system.

Simply minimizing flow rate manipulations is not sufficient to provide acceptable averaging level control. The requirements of averaging level control as stated in Chapter 1 are reiterated here.

- For a given flow disturbance, the manipulated flow rate changes are minimum, i.e. minimize MRCO.
- Maximum surge capacity should be utilized while maintaining the tank level within it maximum and minimum level constraints.
- The manipulated flow rate must be kept within its minimum and maximum constraints.
- After attenuating a disturbance, the tank level must be steered back to its setpoint, i.e. integral action must be present.

MRCO is used as the primary metric in order to compare various control algorithms. The complexity of the solution is taken into consideration as an analytical solution is easier to implement in an industrial computer control system than a numerical solution. The algorithms of interest in this section are PI, CMA, MPCQP, and CMN.

3.2.1 Equivalent Controller Tuning

In order to provide a fair comparison, the algorithms are tuned in the unconstrained case to provide equivalent performances. Time domain measures such as maximum deviation (M_δ) from setpoint, settling time (t_s) and sum of squared error (SSE=$\sum \parallel e(t)^2 \parallel$) are used to assess the closeness of equivalent tuning. Where applicable, design parameters such as prediction and control horizons are set equal.

As previously discussed, the PI controller can be tuned based on the CMA algorithm. In fact, the linear portion of the CMA algorithm is a linear PI controller where the prediction horizon becomes the single tuning parameter. Then it is easy to equivalently tune the PI and CMA controllers. In the case of the MPCQP algorithm, some additional tuning knobs are available. In MPCQP, Q the output weighting matrix and R the input weighting matrix must be appropriately selected to achieve the desired closed loop performance. Finally, in the case of the CMN algorithm, only the prediction horizon is used for tuning. The CMN algorithm provides identical results as CMA when flow constraints are not encountered. Hence, in the unconstrained case, it is also easy to tune CMN by simply defining the same prediction horizon as in CMA. The prediction horizon for the PI, CMA and CMN were fixed at 21. For the MPCQP $N_1 = 1$ and $N_2 = N_u = 21$ with Q and R wights in equal 1 and 90, respectively. With a prediction horizon of 21, the controller utilizes the maximum surge capacity in the unconstrained case without over flowing the tank for the given disturbance of $1.6\,L/min$. A prediction horizon of 21 is also slightly larger than the critical prediction horizon of 20 as defined by equation (2.7), to optimally attenuate the maximum allowable disturbance of $2L/min$. The simulation parameters are set according to Table 3.1. The time domain measures of performance are listed in Table 3.2 and illustrated in Figure 3.2.

Controller	M_δ	t_s	SSE
PI	9.7 cm	9.5 min	2387 cm^2
CMA	9.7 cm	9.5 min	2387 cm^2
MPCQP	9.7 cm	8.5 min	2061 cm^2
CMN	9.7 cm	9.5 min	2387 cm^2

Table 3.2: Unconstrained controller tuning comparison

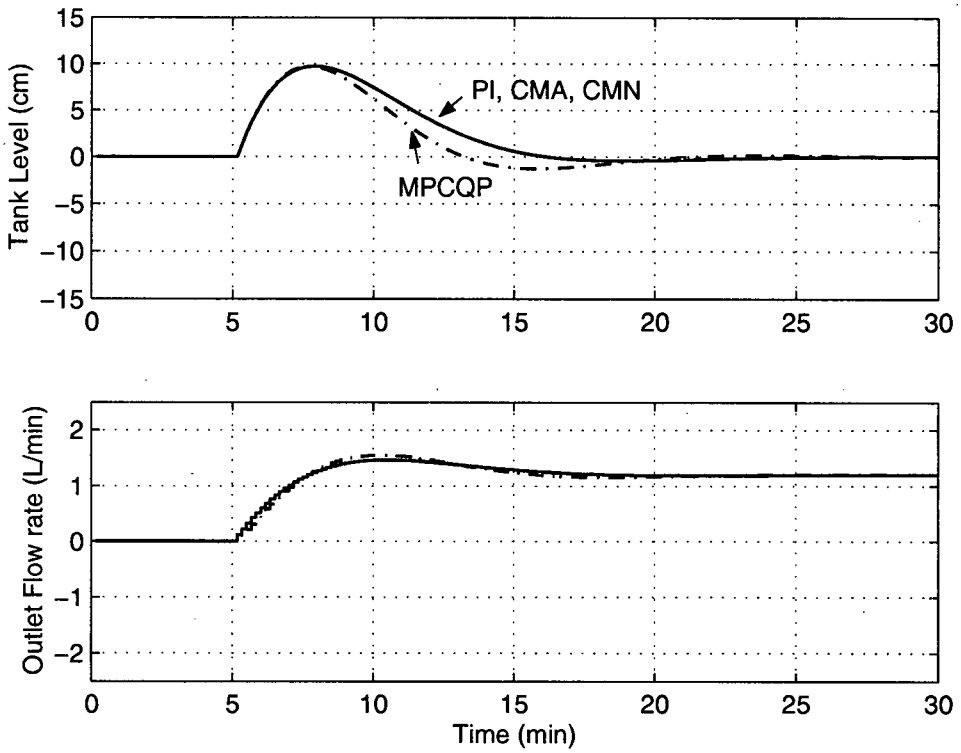

Figure 3.2: Unconstrained controller tuning

The focus of the next section is to provide a comparative analysis between the various algorithms when constraints are defined and evoked using a disturbance magnitude that is 90% of the maximum outlet flow rate.

3.2.2 Case 1: Level Constraints

In this section, only constraints on the tank level are considered. It is assumed that an infinite amount of actuator authority is available. This is not the case in reality as only a finite amount of fluid can be removed from a tank due to the limitation provided by the pump and valve size. The controllers have been tuned as in the unconstrained case and level constraints are introduced. The simulation parameters are as per Table 3.3.

Cross-sectional area, A_c	146.0 cm^2
Nominal level, h	0.0 cm
Maximum level constraint	10.0 cm
Minimum level constraint	- 10.0 cm
Inlet disturbance, q	1.8 L/min

Table 3.3: Simulation parameters: level constraints only

First, the MRCO optimal solution to the single tank problem is presented. As

stated in [12] the optimal control policy is to manipulate the outlet flow rate as a ramp of smallest slope and allowing the level to reach its constraint so the maximum surge capacity is utilized. The optimal solution is computed by minimizing the $\mathcal{L}_\infty$ norm of the outlet flow rate using a infinite horizon controller [12]. The infinite horizon solution can be realized by using a finite horizon controller with a large horizon, as beyond a certain point an additional increase in prediction horizon has no effect on the optimal solution. This can be accomplished by using the CMN algorithm using a prediction horizon of 50. Then the optimal MRCO for $1.8L/min$ load disturbance is $1.24\,L/min/min$ and the result is illustrated in Figure 3.3.

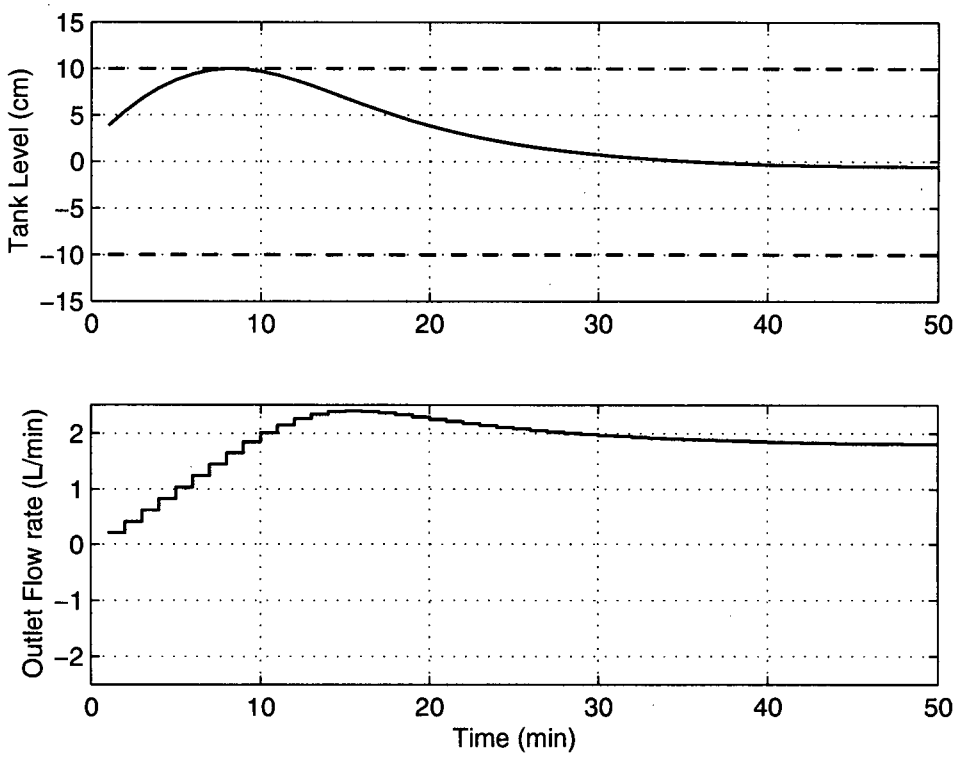

Figure 3.3: SISO MRCO optimal solution

For the proposed algorithms, the simulation results are illustrated in Figure 3.4. The MRCO values for the simulations are displayed in Table 3.4.

Controller	MRCO (L/min/min)
PI	1.03
CMA	1.24
MPCQP	1.59
CMN	1.24
MRCO Optimal	1.24

Table 3.4: MRCO: single tank with level constraints only

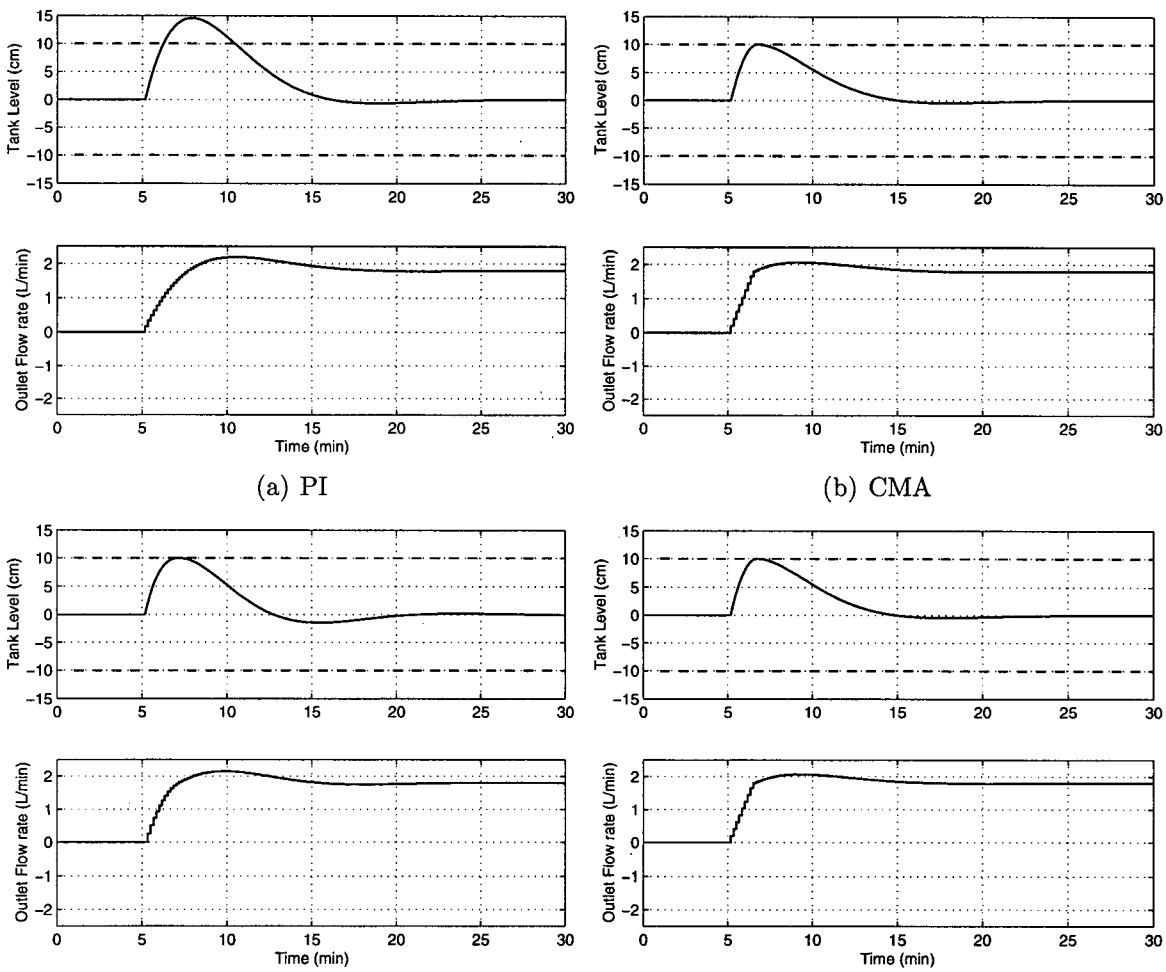

Figure 3.4: Controller comparison: single tank with level constraints only

The PI controller is clearly not able to maintain the tank level within the specified level constraints. This is inherent to the linear PI algorithm as there is no provision for constraint handling. This is the fundamental drawback for utilizing a PI controller for averaging level control.

The CMA algorithm, which is specifically designed to handle state constraints, is able to maintain the tank level within its limits. The optimal policy is to manipulate the outlet flow rate as a ramp of the smallest slope. The slope of the ramp must be such that the inlet flow disturbance is exactly matched as the tank level reaches its limit [12]. The CMA controller exhibits this optimal ramp behavior along with exerting additional control effort to bring the level to setpoint. The tank level is returned to the origin in about $3.0 \cdot P$ sample times or approximately 8.75 minutes. Additionally, as the $\mathcal{L}_\infty$ norm on ∇u is explicitly minimized, the CMA exhibits the MRCO optimal solution, while satisfying level constraints, as seen in Table 3.4.

MPCQP is also able to handle tank level constraints. As MPCQP minimizes the

$\mathcal{L}_2$ norm on ∇u, similar to minimizing the averaging control energy, minimum MRCO is not guaranteed. But when compared to the optimal MRCO, the MPCQP solution is not significantly larger. The drawback of MPCQP in this scenario is that on-line optimization via QP is required, whereas CMA has an analytical solution that is MRCO optimal.

The CMN algorithm produces identical results as CMA in the case when only level constraints are defined. The interpretation of results for the CMN algorithm are identical to the CMA algorithm. The fundamental difference between the two algorithms is that the control action in CMN is produced by solving an on-line LP optimization. The LP optimization needlessly increases solution complexity when CMA can produce identical results.

3.2.3 Case 2: Level & Flow Constraints

In this section, a more realistic scenario is presented. Every actuator has minimum and maximum limits. A 'good' control strategy must consider such limitations, or controller windup may result. Here, both level and flow rate constraints are defined, and the simulations are set up as per Table 3.3. Flow rate constraints of ± 2.0 L/min were defined and a disturbance of 1.8 L/min was introduced. The simulation results are illustrated in Figure 3.5 and the corresponding MRCO values are listed in Table 3.5.

Controller	MRCO (L/min/min)
PI	1.03
CMA	1.24
MPCQP	1.59
CMN	3.59
MRCO Optimal	1.24

Table 3.5: MRCO: single tank with level and flow rate constraints

The PI controller can be augmented with an anti-windup circuit, as shown in section (2.1), to prevent actuator constraint violations. The PI controller is still unable to handle level constraints. A PI controller tuned for averaging level control is clearly not the best control policy. Regardless of the method chosen for tuning a PI controller, it cannot guarantee to maintain the level within the specified constraints. This clearly puts the PI algorithm at a disadvantage, therefore, it will not be further discussed in the multivariable framework.

The CMA algorithm is able to handle flow rate constraints. However, unlike the PI algorithm, the CMA is also able to handle level constraints. The only difference in performance by introducing flow rate constraints is that the settling time is slightly

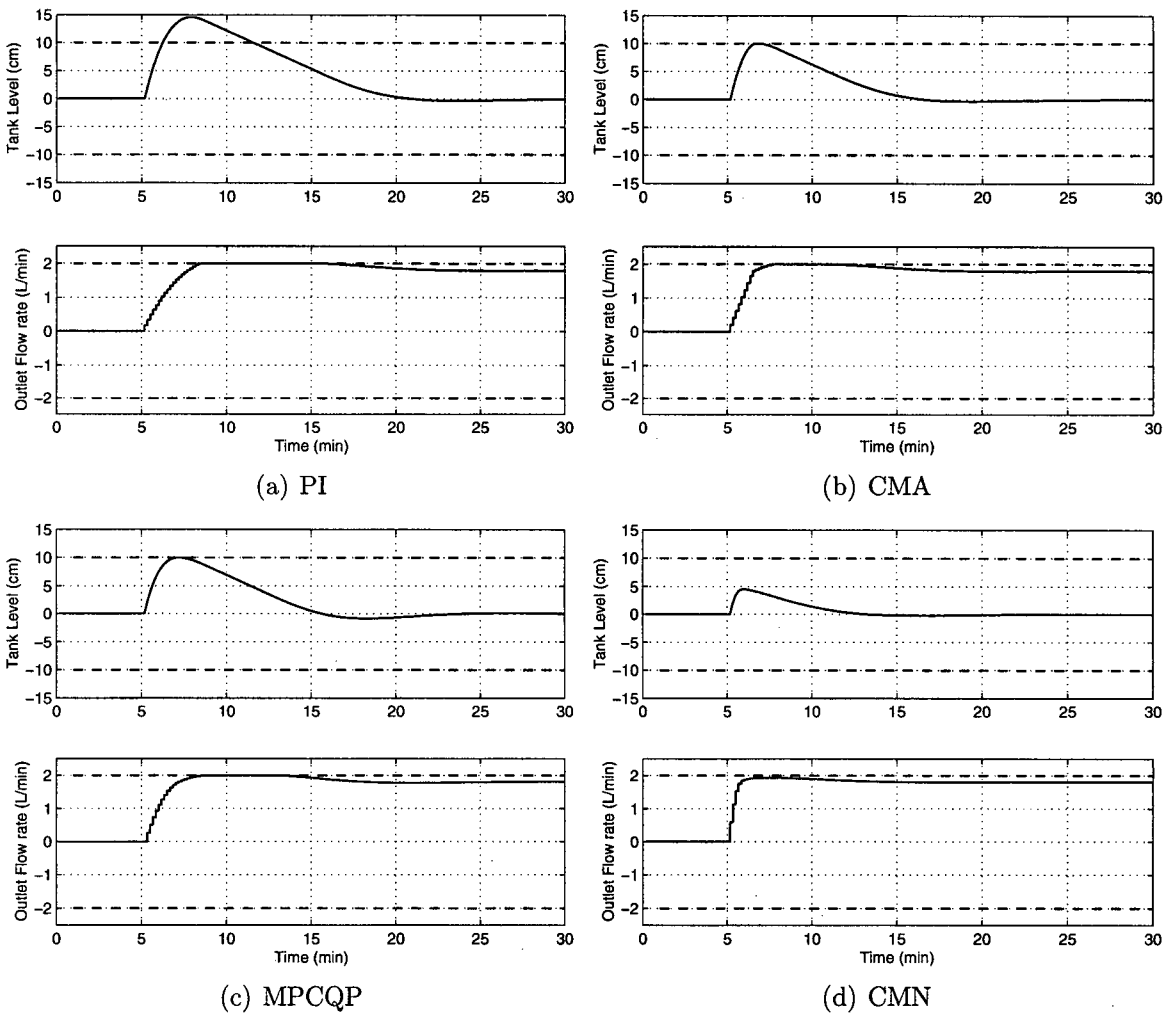

Figure 3.5: Controller comparison: single tank with level and flow constraints

increased. The MRCO value is still optimal as supported by Theorem 2.1.

Similarly, the MPCQP algorithm is able to handle both level and flow rate constraints. Even though both level and flow rate constraints become active during the simulation, the degradation in controller performance is minimal. The settling time increases slightly but the MRCO values is not effected, compare Table 3.4 and Table 3.5.

In the case of CMN, the algorithm is unable to utilize the full surge capacity as the outlet flow rate is aggressively manipulated. Such manipulations have the adverse effect of inflating the MRCO value by about three times as shown in Table 3.5. Although the algorithm is able to maintain both tank level and outlet flow rate within their respective constraints, it is not MRCO optimal. This result can be attributed to the use of terminal constraints to induce integral action as formulated in equation (2.2). In the CMN formulation, it is required that, at the end of the prediction horizon the level must be at its desired value. In the presence of a flow rate constraint, such a requirement is not possible while allowing the smallest change to the flow rate. Hence, the terminal constraint dom-

inates the optimization result and defeats the flow filtering objective. In the presence of all process and terminal constraints, the solution is still optimal in the $\mathcal{L}_\infty$ sense but not desirable.

3.3 MIMO Averaging Level Control

In this section, the case of the interconnected multiple tank system is discussed. It is of interest to explore how controller performance is affected as the degree of coupling is varied. For the case where recycle fraction is 0%, the two-tank system is inherently decoupled. Then using decentralized control is sufficient as discussed in the previous section. In this section moderate coupling, 40% recycle fraction, and strong coupling, 70% recycle fraction, are analyzed.

The tuning of a MIMO MPC can be a cumbersome task as there are no concrete tuning guidelines. The effects and interactions of various tuning knobs are not well understood. In order to alleviate this problem and provide a baseline for comparison, the various multivariable controllers have been tuned as in the single tank case. The MRCO for the multivariable system is defined as $\sum_{i=1}^{m} \parallel \nabla U_i \parallel_\infty$.

It is important that neither of the two tanks violate their lower and upper constraints. The level constraints of each tank can be defined independently, but for ease of comparison the level constraints on each tank are defined to be identical. The system is simulated using parameters as defined in Table 3.6.

	Tank 1	Tank 2
Cross-sectional area, A_c	146.0 cm^2	146.0 cm^2
Nominal level,h	0.0 cm	0.0 cm
Maximum level constraint	10.0 cm	10.0 cm
Minimum level constraint	-10.0 cm	-10.0 cm
Inlet disturbance q,$f_1 = f_2 = 40\%$	1.6 L/min	0.0 L/min
Inlet disturbance q,$f_1 = f_2 = 70\%$	0.9 L/min	0.0 L/min

Table 3.6: MIMO simulation parameters: level constraints only

Again, prior to presenting the simulation results using the various algorithms the optimal MRCO solution is established. As previously, the optimal MRCO solution can be realized using the CMN algorithm with a sufficiently large prediction horizon of 50. For the 40% and 70% recycle fractions the results are shown in Figure 3.6 and the optimal MRCO values are 0.99 $L/min/min$ and 0.56 $L/min/min$, respectively.

This section is arranged such that level constraints are first considered and then followed by the more complete case where both level and flow rate constraints are addressed.

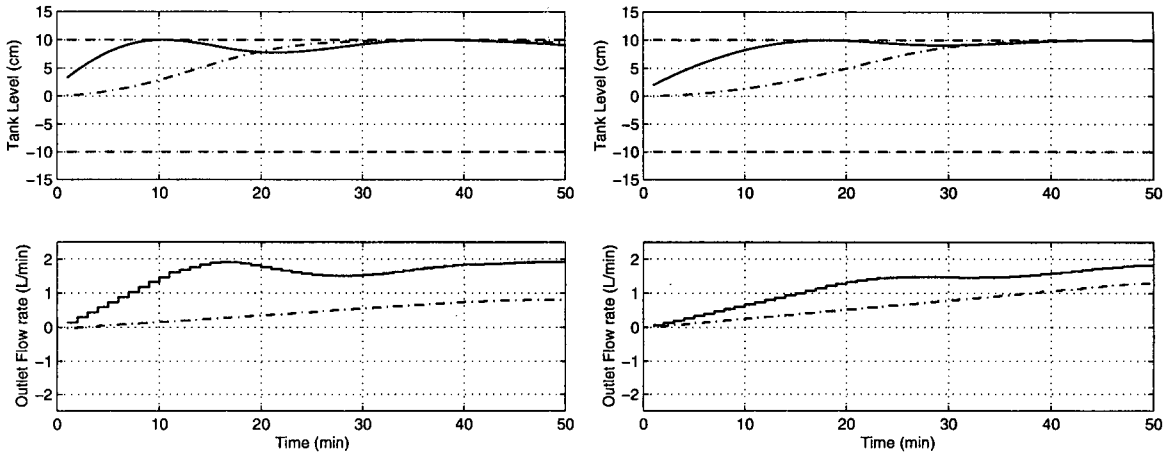

(a) 40% Recycle (b) 70% Recycle

Figure 3.6: MIMO optimal MRCO, Tank 1 (solid) Tank 2 (dash-dot)

The effect of coupling in the system is discussed within each scenario.

3.3.1 Case 1: Level Constraints

The control algorithms of interest in the multiple tank case are Decentralized CMA, Decoupled CMA, MPCQP and CMN. In this section, the PI control algorithm has been discarded due to its inability to handle level constraints. As previously mentioned, comparison of the various controllers is further complicated due to the inherit coupling in the system. Figure 3.7 illustrates the closed-loop response with the various control algorithms for the 40% recycle case and Figure 3.8 exhibits the close loop response for the 70% recycle case. The MRCO values are summarized in Table 3.7.

	MRCO (L/min/min)	
Controller	$f_1 = f_2 = 40\%$	$f_1 = f_2 = 70\%$
Decentralized CMA	2.02	0.82
Decoupled CMA	1.89	1.79
MPCQP	1.34	0.69
CMN	1.51	1.71
MRCO Optimal	0.99	0.56

Table 3.7: MRCO: two-tank system with level constraints

For the given step disturbance in tank 1, Decentralized CMA is unable to handle the level constraints. The CMA algorithm is based on the assumption that the step disturbance will persist for the entire prediction horizon. But in the multi-tank system, due to system coupling, the step disturbance which enters tank 1 becomes a ramp disturbance to tank 2 and, furthermore, makes its way back to tank 1 as a ramp disturbance. As the

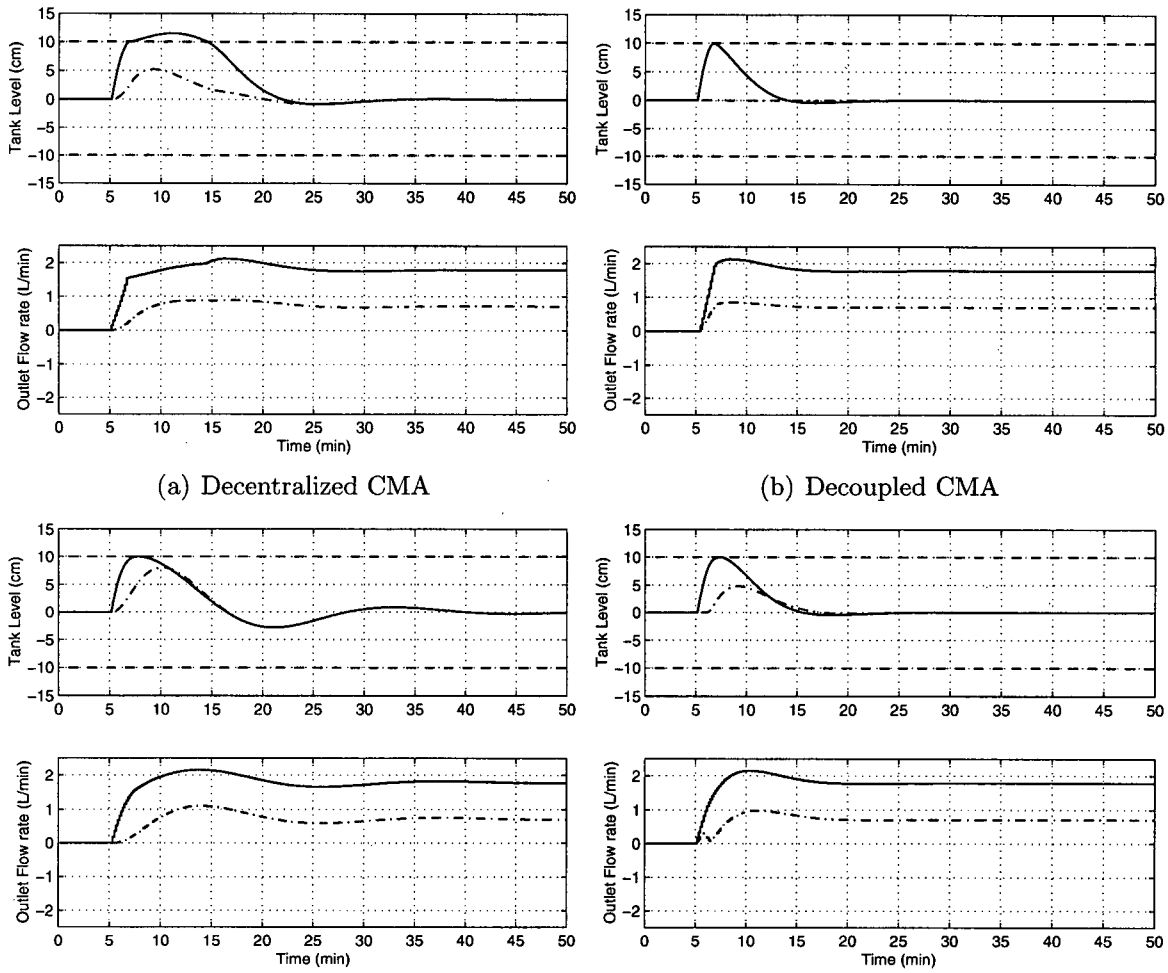

(a) Decentralized CMA

(b) Decoupled CMA

(c) MPCQP

(d) CMN

Figure 3.7: Controller comparison: two-tank system with level constraints for $f_1 = f_2 = 40\%$, Tank 1 (solid) Tank 2 (dash-dot)

ramp disturbance violates the fundamental disturbance assumption in CMA, the controller is unable to maintain the tank level within the specified constraints. Similar behavior is observed when the recycle fraction is increased to 70%.

Level constraints are not violated for the Decoupled CMA algorithm. Assuming a perfect plant model is known, the decoupled controller will guarantee that level constraints are never violated as stated by Theorem 2.2. The main drawback of this strategy is that the total surge capacity in the system cannot be utilized for flow smoothing. As can be seen in both Figure 3.7 and Figure 3.8, in order to provide decoupling, the control strategy ramps the outlet flow rate of tank 2 at the rate which matches the load disturbance and allows no deviation in the level of tank 2. This prevents the surge capacity of the second tank from being used for flow smoothing. This leads to the algorithm not being MRCO optimal as compared in Table 3.7. However this simple strategy provides reasonable results.

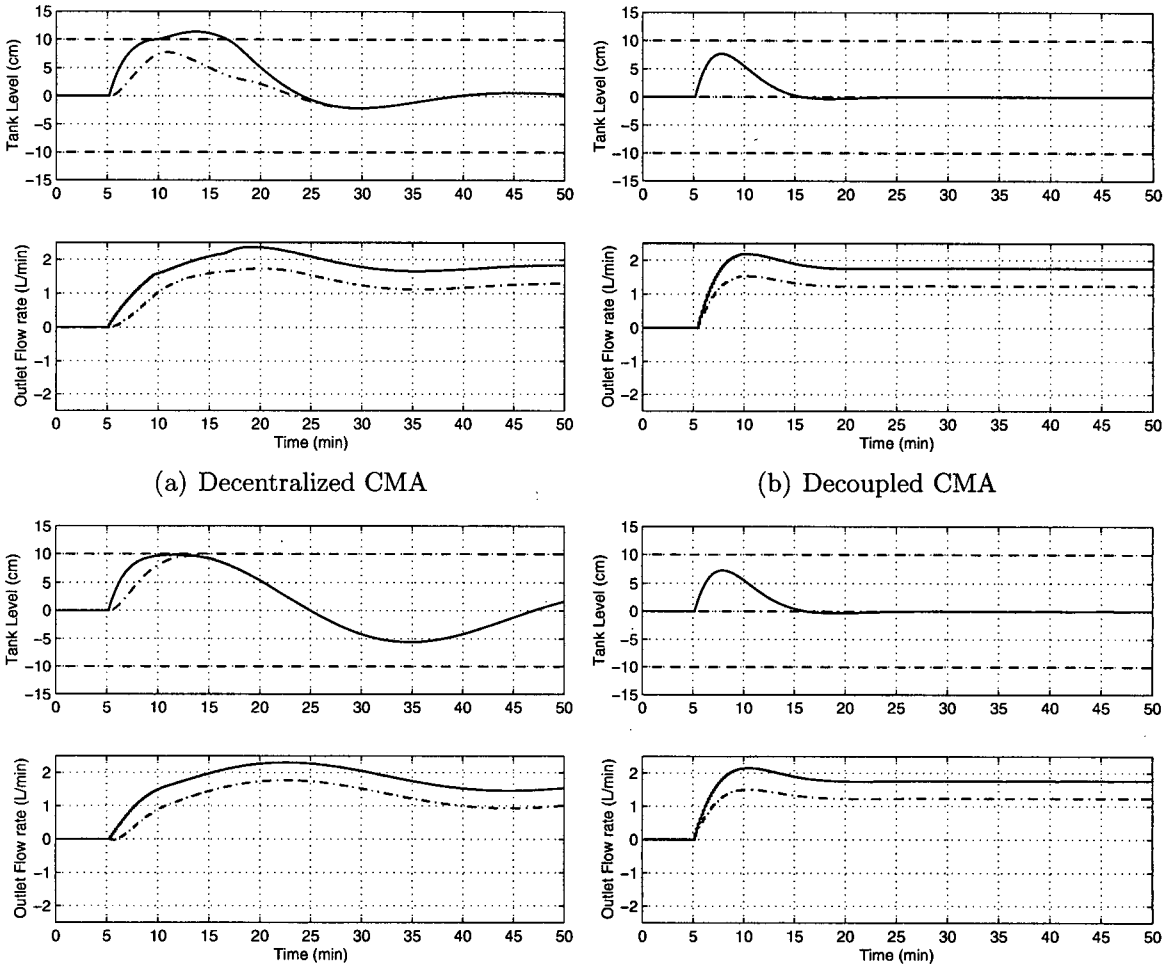

(a) Decentralized CMA

(b) Decoupled CMA

(c) MPCQP

(d) CMN

Figure 3.8: Controller comparison: two-tank system with level constraints for $f_1 = f_2 = 70\%$, Tank 1 (solid) Tank 2 (dash-dot)

Illustrated in Figure 3.7(c) and Figure 3.8(c) are the responses of the MPCQP control algorithm under various degrees of system coupling. In addition to effectively handling the level constraints, this control algorithm uses almost all the surge capacity. Minimal changes are made to the outlet flow rates of both tanks as the load disturbance is transferred to the tank levels. MPCQP is not MRCO optimal but provides the smallest MRCO when compared to other algorithms. Furthermore, the closed-loop response becomes oscillatory and the settling time increases as the amount of coupling in the process is increased.

As in the MPCQP case, the CMN algorithm was also tuned based on the unconstrained case. As it can be seen in Figure 3.7, the CMN algorithm also tries to make use of the capacity of both tanks in the 40% case. But the sensitivity of CMN to tuning is clearly illustrated when the recycle fraction is increased to 70%. The CMN algorithm essentially decouples the system and as a result does not utilize maximum available surge

capacity. The primary reason for such behavior is the definition of terminal constraints and the length of the prediction horizon. The controller becomes short sighted and takes much more aggressive actions, making it suboptimal in the MRCO sense.

3.3.2 Case 2: Level & Flow Constraints

In this section, the more complete case including both level and flow rate constraints is compared. Figure 3.9 and 3.10 show the closed-loop response of the two-tank system for recycle fractions of 40% and 70%, respectively and the MRCO values are compared in Table 3.8. As before, each actuator is limited to a flow rate of $\pm 2\ L/min$.

The Decentralized CMA is able to handle flow rate constraints but cannot handle level constraints. Again, the disturbance assumption for CMA is violated and, as a result, CMA is unable to handle level constraints. It is interesting to note that even though the controller is unable to guarantee level constraint handling, the controller is still aware of the constraints and tries to be pre-emptive. The controller does attempt to compensate for the underestimation of the flow disturbance, but obviously the strategy is not MRCO optimal as shown in Table 3.8.

	MRCO (L/min/min)	
Controller	$f_1 = f_2 = 40\%$	$f_1 = f_2 = 70\%$
Decentralized CMA	2.02	0.82
Decoupled CMA	1.89	1.91
MPCQP	1.34	0.69
CMN	3.69	3.65
MRCO Optimal	0.99	0.56

Table 3.8: MRCO: two-tank system with level and flow rate constraints

In the case of the Decoupled CMA, somewhat different results are obtained when flow rate constraints are introduced. Since one of the requirements of Theorem 2.2 is violated, the Decoupled CMA is no longer guaranteed to handle level constraints. The requirement that sufficient control authority is available for decoupling and control is violated. Since there is only a finite control authority the system is not fully decoupled [7]. This can be seen in Figure 3.9 and, to a greater extent, in Figure 3.10; when the tank 1 flow rate saturates, the tank 2 level is no longer perfectly decoupled. The partial coupling in the system also implies that the disturbance assumption in CMA is violated. The CMA controller in the partially decoupled space experiences ramp type disturbances which lead to level constraint violations as clearly seen in Figure 3.10(b).

The MPCQP algorithm is able to handle all system constraints. The level and flow rate constraints are handled quite easily without much degradation in the closed-

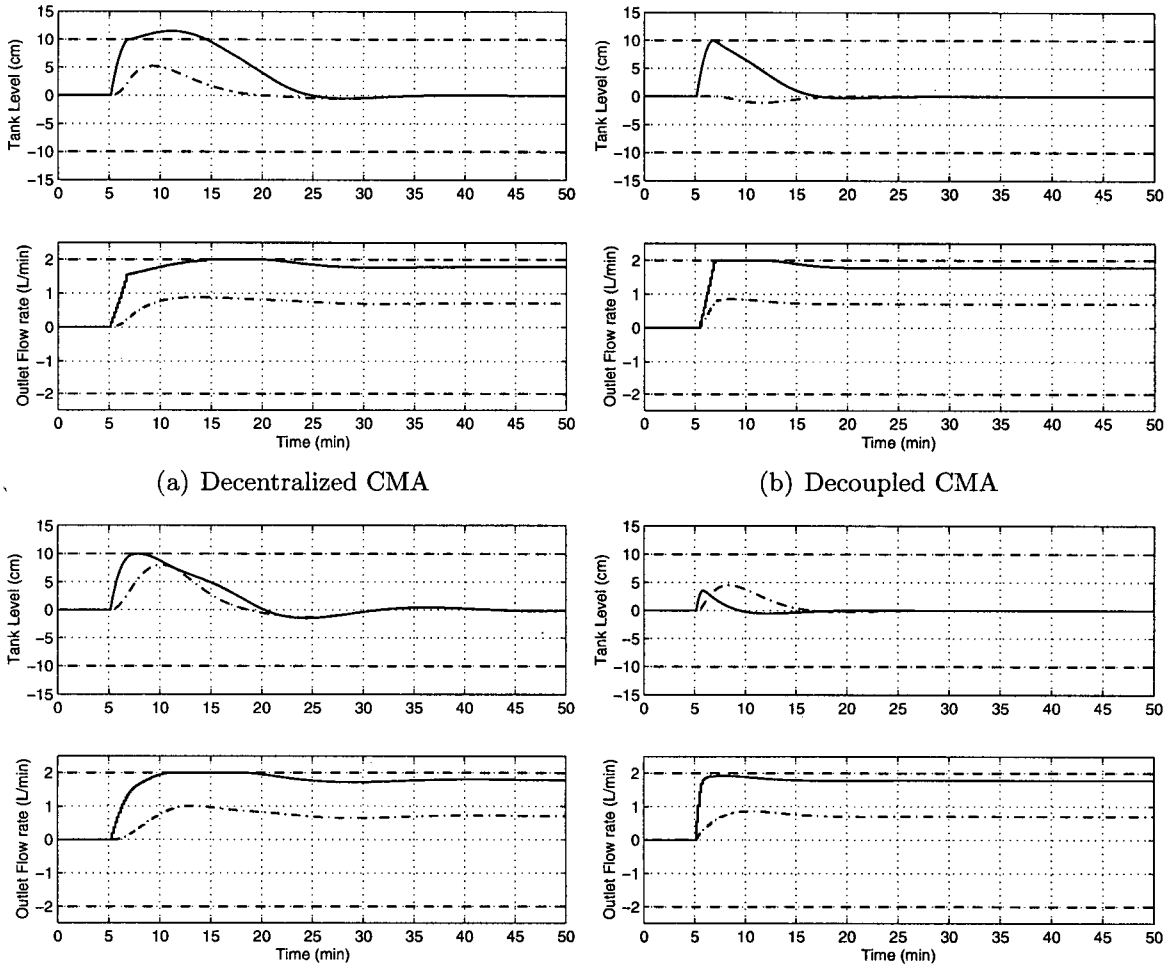

(a) Decentralized CMA

(b) Decoupled CMA

(c) MPCQP

(d) CMN

Figure 3.9: Controller comparison: two-tank system with level constraints for $f_1 = f_2 = 40\%$, Tank 1 (solid) Tank 2 (dash-dot)

loop performance. The controller attempts to utilize the maximum surge capacity to attenuate inlet flow disturbances. Furthermore, there is no change in the MRCO value when flow rate constraints are introduced, suggesting that the algorithm is not sensitive to tuning. Actually, by introducing flow rate constraints, the closed-loop response becomes less oscillatory. This can be attributed to the fact that the control authority is limited hence large overshoot on the control action are prevented. Even though MPCQP is not MRCO optimal, it is able to provide the smallest MRCO value as shown in Table 3.8.

Again, the CMN algorithm is unable to provide MRCO optimal control. The controller becomes extremely aggressive when flow rate constraints are introduced. From Figure 3.10 it can be observed that the flow filtering objective is clearly defeated but the terminal constraint requirements are satisfied. From the closed-loop simulations in the SISO and MIMO cases, it can also be observed that the response is effected by flow rate constraints, terminal constraints, load disturbance magnitude and process coupling. For

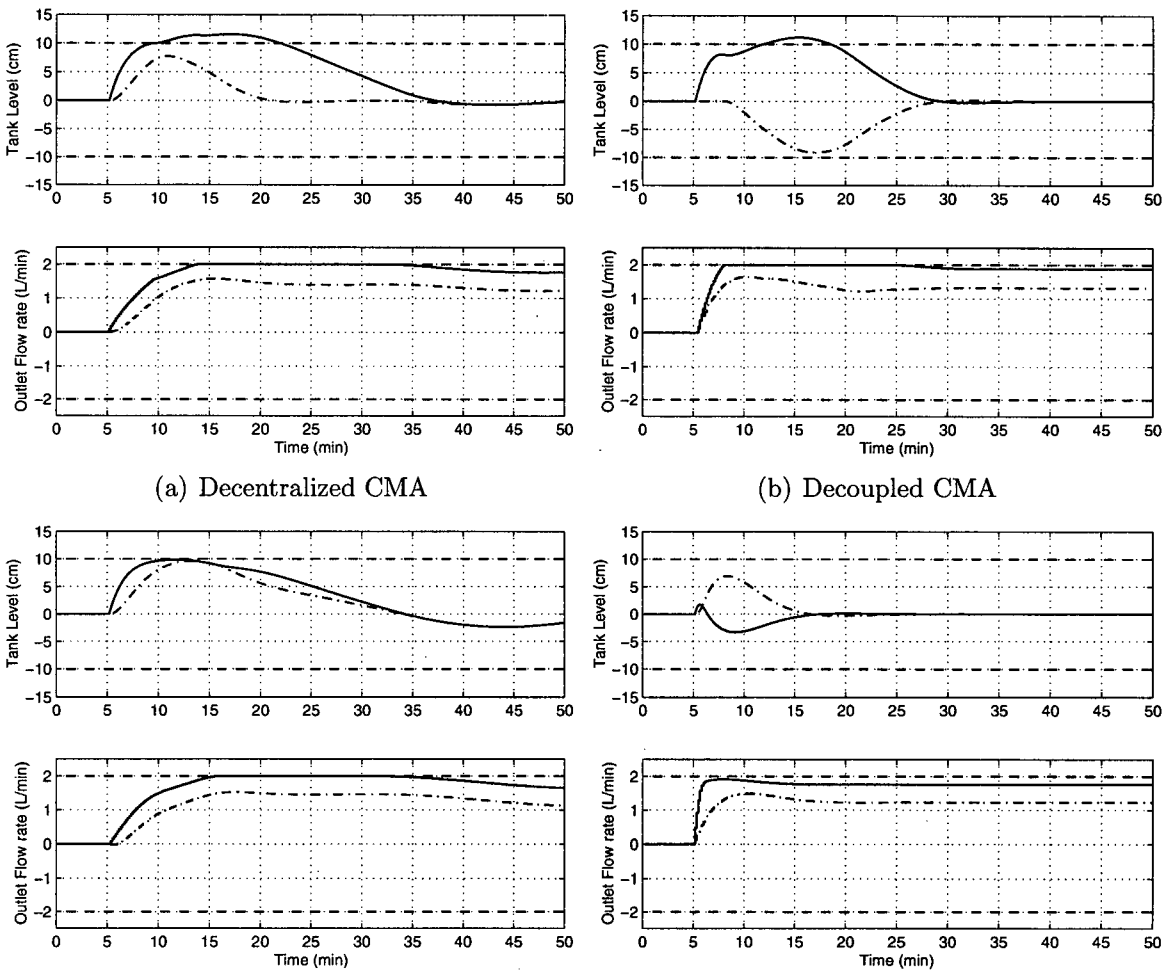

(a) Decentralized CMA

(b) Decoupled CMA

(c) MPCQP

(d) CMN

Figure 3.10: Controller comparison: two-tank system with level and flow constraints for $f_1 = f_2 = 70\%$, Tank 1 (solid) Tank 2 (dash-dot)

the CMA algorithm, equation (2.7) shows that prediction horizon must be greater than the critical horizon in order to remove the effect of terminal constraint and achieve MRCO optimality. Likewise, a similar condition may exist for the MIMO CMN, which leads to the following conjecture.

Conjecture 3.1. *For the MIMO CMN algorithm there exists a control horizon, larger than that computed in the SISO case, which is a function of level constraints, flow rate constraints, load disturbance and system interaction that would provide MRCO optimal control.*

The above conjecture is directly supported by the MRCO optimal solution where a prediction horizon of 50 was found to be optimal. This suggests that the CMN algorithm is very sensitive to tuning.

3.4 Chapter Reflections

This chapter has been dedicated to providing a rigorous comparison between various control algorithms designed for averaging level control. For the single tank system, it was demonstrated that the CMA algorithm is sufficient to guarantee both level and flow rate constraints. The results are summarized in Table 3.9.

Controller	Level Constraint	Level & Flow Rate Constraint	Features
PI	×	×	• Handles constraints
	✓	✓	• MRCO optimal
	Analytical	*Analytical*	• Solution Complexity
CMA	✓	✓	• Handles constraints
	✓	✓	• MRCO optimal
	Analytical	*Analytical*	• Solution Complexity
MPCQP	✓	✓	• Handles constraints
	×	×	• MRCO optimal
	Numerical	*Numerical*	• Solution Complexity
CMN	✓	✓	• Handles constraints
	✓	×	• MRCO optimal
	Numerical	*Numerical*	• Solution Complexity

Table 3.9: SISO simulation comparison results

The situation is much more complicated for the multiple tank system. It was shown that the approach of applying decentralized CMA controllers results in level constraint violation. The Decoupled CMA and MPCQP provided the best results for the two-tank system. The Decoupled CMA algorithm guarantees level constraint handling provided no flow rate

Controller	Level Constraint	Level & Flow Rate Constraint	Features
Decentralized CMA	×	×	• Handles constraints
	×	×	• MRCO optimal
	Analytical	*Analytical*	• Solution Complexity
Decoupled CMA	✓	×	• Handles constraints
	×	×	• MRCO optimal
	Analytical	*Analytical*	• Solution Complexity
MPCQP	✓	✓	• Handles constraints
	×	×	• MRCO optimal
	Numerical	*Numerical*	• Solution Complexity
CMN	✓	✓	• Handles constraints
	×	×	• MRCO optimal
	Numerical	*Numerical*	• Solution Complexity

Table 3.10: MIMO simulation comparison results

constraints are encountered. When one of the actuators does saturate, the decoupling is no longer perfect and level constraint violation may result. When ample computational resources are available, implementing the MPCQP algorithm would serve as the best strat-

egy for the MIMO case. The MPCQP algorithm has excellent characteristics as it is able to maintain the system within specified constraints and, most importantly, provides the lowest MRCO for the chosen simulation scenario. It was also demonstrated that the CMN algorithm has some severe drawbacks when flow rate constraints are introduced, making the controller near-sighted. This occurs in both the SISO and MIMO cases. It was conjectured that this problem might be overcome by increasing the prediction horizon, but there is no guarantee that the same problem will not occur under a different scenario. The simulation results for the MIMO case are summarized in Table 3.10.

However, the MPC formulation that explicitly minimizes the MRCO is still very attractive. Thus, the objective of the next chapter is to mitigate the problem with the CMN algorithm by proposing a novel mixed norm algorithm.

Chapter 4

$\mathcal{L}_1/\mathcal{L}_\infty$ MPC: Mixed Norm Formulation

It was shown in Chapter 3 that the MPC formulation using the $\mathcal{L}_\infty$ norm with terminal constraints, CMN, had some undesirable properties when flow rate constraints were introduced. It was observed that the integral action via terminal constraints became a competing objective with minimizing the MRCO. On the other hand, the MPC formulation using the $\mathcal{L}_2$ norm, MPCQP was quite insensitive to flow rate constraints and actually provided the better result. The objective of this chapter is to present a variation of the CMN algorithm, called $\mathcal{L}_1/\mathcal{L}_\infty$ MPC, that mitigates some of the drawbacks in the original formulation. In addition, utilizing LP optimization for constrained MPC is analyzed and compared with the QP algorithm.

4.1 $\mathcal{L}_1/\mathcal{L}_\infty$ MPC Theory and Design

The requirement that the tank level must be at its setpoint at the end of the prediction horizon can be problematic. MPC is a receding horizon control strategy in which only the first of the computed control actions is implemented and the problem is re-evaluated at the next sample time. A more realistic requirement is that as time goes on, the level deviation from setpoint due to a disturbance or the control error should approach zero. In the $\mathcal{L}_1/\mathcal{L}_\infty$ MPC, the terminal constraint is removed by penalizing the sum of absolute deviations from setpoint. This can be accomplished by penalizing the $\mathcal{L}_1$ norm of the error. But in order to explicitly minimize the MRCO, it is still desirable to penalize the ∇u in the $\mathcal{L}_\infty$ norm sense. By combining $\mathcal{L}_1$ and $\mathcal{L}_\infty$ norms, both objectives can be met and the problem can be solved using LP optimization. The following gives the details for constructing the mixed norm algorithm.

The cost function to be minimized is defined as

$$J(k) = \sum_{j=N_2}^{N_2} \mid y(k+j) - r(k+j) \mid_Q + \sum_{i=1}^{m} \parallel \nabla U_i \parallel_R^\infty$$

subject to: (4.1)

$$y_{min} \leq y(k) \leq y_{max}$$

$$u_{min} \leq u(k) \leq u_{max}$$

where the minimization is defined over $\Re^{mN_u}$. The cost function is formulated as to

penalize the control errors at the end of the prediction horizon. Within this framework the algorithm gives greater precedence to minimizing the MRCO rather than minimizing the control error. This setup is also favourable as the largest magnitude of the control actions are computed in the first few elements of each prediction.

The augmentation of the state-space model along with setting up the prediction matrices is analogous to that defined in section 2.3. Similarly, the constraints on the input magnitudes, input slew rates and on the states can be defined as before.

In order to formulate $\mathcal{L}_1/\mathcal{L}_\infty$ MPC as a LP optimization, the following change of variables is performed.

For series of $\eta \geq 0$ and $\mu \geq 0$, redefine the cost function as

$$\begin{array}{rcccl} -\eta & \leq & y(k+j) - r(k+j) & \leq & \eta \\ -\mu & \leq & \nabla U(k+j-1) & \leq & \mu \\ 0 & \leq & \mathcal{M}\mathcal{Q}\eta_i + \mathcal{H}\mathcal{R}\mu_i & \leq & \pi \end{array} \tag{4.2}$$

where $\mathcal{M}$ is defined as

$$\mathcal{M} = \begin{bmatrix} \mathbf{0} & \cdots & \mathbf{0} \\ \vdots & \ddots & \vdots \\ \mathbf{1}_p^T & \cdots & \mathbf{1}_p^T \end{bmatrix}$$

Then π becomes the upper bound for the original cost function. The problem can now be

cast in the LP optimization framework.

$$\min_{\pi\,\mu\,\eta\,\nabla U} \pi$$

subject to:

$$\begin{aligned}
\eta &\geq \mathcal{C}\mathcal{F}\xi(k) + \mathcal{C}\mathcal{G}\nabla U - \overline{r}(k) \\
\eta &\geq -\mathcal{C}\mathcal{F}\xi(k) - \mathcal{C}\mathcal{G}\nabla U + \overline{r}(k) \\
\delta &\geq \mathcal{F}\xi(k) + \mathcal{G}\nabla U \\
-\gamma &\geq -\mathcal{F}\xi(k) - \mathcal{G}\nabla U \\
\mu &\geq \nabla U \\
\mu &\geq -\nabla U \\
\omega &\geq \nabla U \\
\mathbf{0} &\geq -\nabla U + \psi \\
\beta &\geq \Lambda\nabla U(k) + \mathcal{I}u(k-1) \\
-\alpha &\geq -\Lambda\nabla U(k) - \mathcal{I}u(k-1) \\
\pi &\geq \mathcal{M}\mathcal{Q}\mu_i + \mathcal{H}\mathcal{R}\eta_i
\end{aligned}$$

The above optimization problem can then be rearranged into the standard LP form by defining $\overline{\nabla U} = \nabla U - \psi$:

$$\min_{\mathbf{x}} \mathbf{c}^T\mathbf{x}$$

subject to

$$\begin{aligned} \mathbf{A}\mathbf{x} &\leq \mathbf{b} \\ \mathbf{x} &\geq \mathbf{0} \end{aligned} \tag{4.3}$$

where

$$\mathbf{c} = \begin{pmatrix} \mathbf{0} \\ \mathbf{0} \\ \mathbf{0} \\ 1 \end{pmatrix} \qquad \mathbf{x} = \begin{pmatrix} \overline{\nabla U} \\ \eta \\ \mu \\ \pi \end{pmatrix}$$

$$\mathbf{A} = \begin{pmatrix} \mathcal{C}\mathcal{G} & -\mathbf{I} & \mathbf{0} & \mathbf{0} \\ -\mathcal{C}\mathcal{G} & -\mathbf{I} & \mathbf{0} & \mathbf{0} \\ \mathcal{G} & \mathbf{0} & \mathbf{0} & \mathbf{0} \\ -\mathcal{G} & \mathbf{0} & \mathbf{0} & \mathbf{0} \\ \mathbf{I} & \mathbf{0} & -\mathbf{I} & \mathbf{0} \\ -\mathbf{I} & \mathbf{0} & -\mathbf{I} & \mathbf{0} \\ \mathbf{I} & \mathbf{0} & \mathbf{0} & \mathbf{0} \\ \Lambda & \mathbf{0} & \mathbf{0} & \mathbf{0} \\ -\Lambda & \mathbf{0} & \mathbf{0} & \mathbf{0} \\ \mathbf{0} & \widetilde{Q} & \widetilde{R} & -\mathbf{1} \end{pmatrix} \qquad \mathbf{b} = \begin{pmatrix} -\mathcal{C}\mathcal{G}\psi - \mathcal{C}\mathcal{F}\xi(k) + \overline{r}(k) \\ \mathcal{C}\mathcal{G}\psi + \mathcal{C}\mathcal{F}\xi(k) - \overline{r}(k) \\ \delta - \mathcal{G}\psi - \mathcal{F}\xi(k) \\ \gamma - \mathcal{G}\psi - \mathcal{F}\xi(k) \\ -\phi \\ \omega \\ \omega - \phi \\ \beta - \Lambda\phi - \mathcal{I}u(k-1) \\ -\alpha + \Lambda\phi + \mathcal{I}u(k-1) \\ 0 \end{pmatrix}$$

This formulation removes the restrictive end point constraint while ensuring control error minimization. In addition, the algorithm explicitly minimizes the $\mathcal{L}_\infty$ norm on ∇U, which is desirable for averaging level control.

4.2 Controller Comparison: Simulation Results

It is now interesting to compare $\mathcal{L}_1/\mathcal{L}_\infty$ MPC with some of the controllers from the previous chapter. It was shown that the behaviour of the CMN algorithm was undesirable when tank level and flow rate constraints were introduced. The degradation in performance was apparent in the SISO case and even more so in the MIMO case. The $\mathcal{L}_1/\mathcal{L}_\infty$ MPC aims to alleviate this problem while continuing to use LP optimization. As in the previous chapter, first the $\mathcal{L}_1/\mathcal{L}_\infty$ MPC is equivalently tuned in the unconstrained SISO

case. The comparative simulation was set up according to Table 3.1. In tuning the $\mathcal{L}_1/\mathcal{L}_\infty$ MPC, the prediction and control horizons were chosen to be 21 samples as before, while the weights were set as $Q = 1$ and $R = 160$. The tuning results are displayed in Figure 4.1 and time domain metrics are stated in Table 4.1.

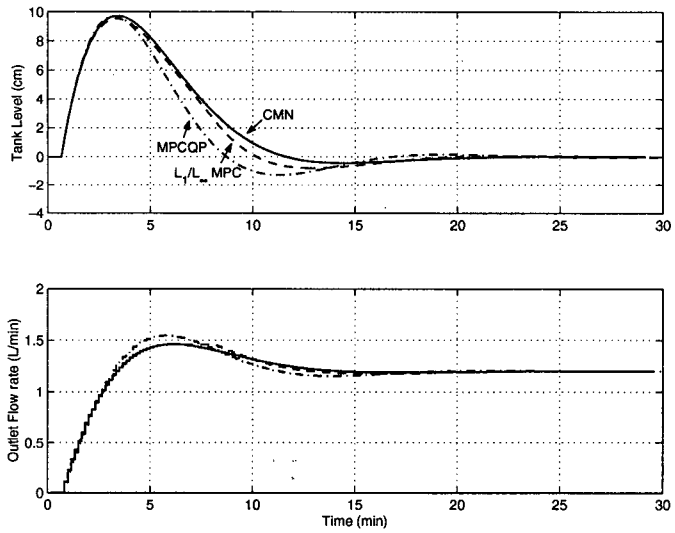

Figure 4.1: Unconstrained controller comparison

Controller	M_δ	t_s	SSE
CMA	9.7 cm	9.5 min	2387 cm^2
MPCQP	9.7 cm	8.5 min	2061 cm^2
CMN	9.7 cm	9.5 min	2387 cm^2
$\mathcal{L}_1/\mathcal{L}_\infty$ MPC	9.6 cm	9.0 min	2249 cm^2

Table 4.1: Unconstrained controller tuning comparison

In this section, comparisons are made when both level and flow rate constraints are defined. For the single tank case, the simulation again was set up according to Table 3.3. The results are illustrated in Figure 4.2 where the closed-loop performances with CMA, MPCQP, CMN and $\mathcal{L}_1/\mathcal{L}_\infty$ MPC are illustrated.

Controller	MRCO (L/min/min)
CMA	1.24
MPCQP	1.59
CMN	3.59
$\mathcal{L}_1/\mathcal{L}_\infty$ MPC	1.24
MRCO Optimal	1.24

Table 4.2: MRCO: single tank with level and flow rate constraints

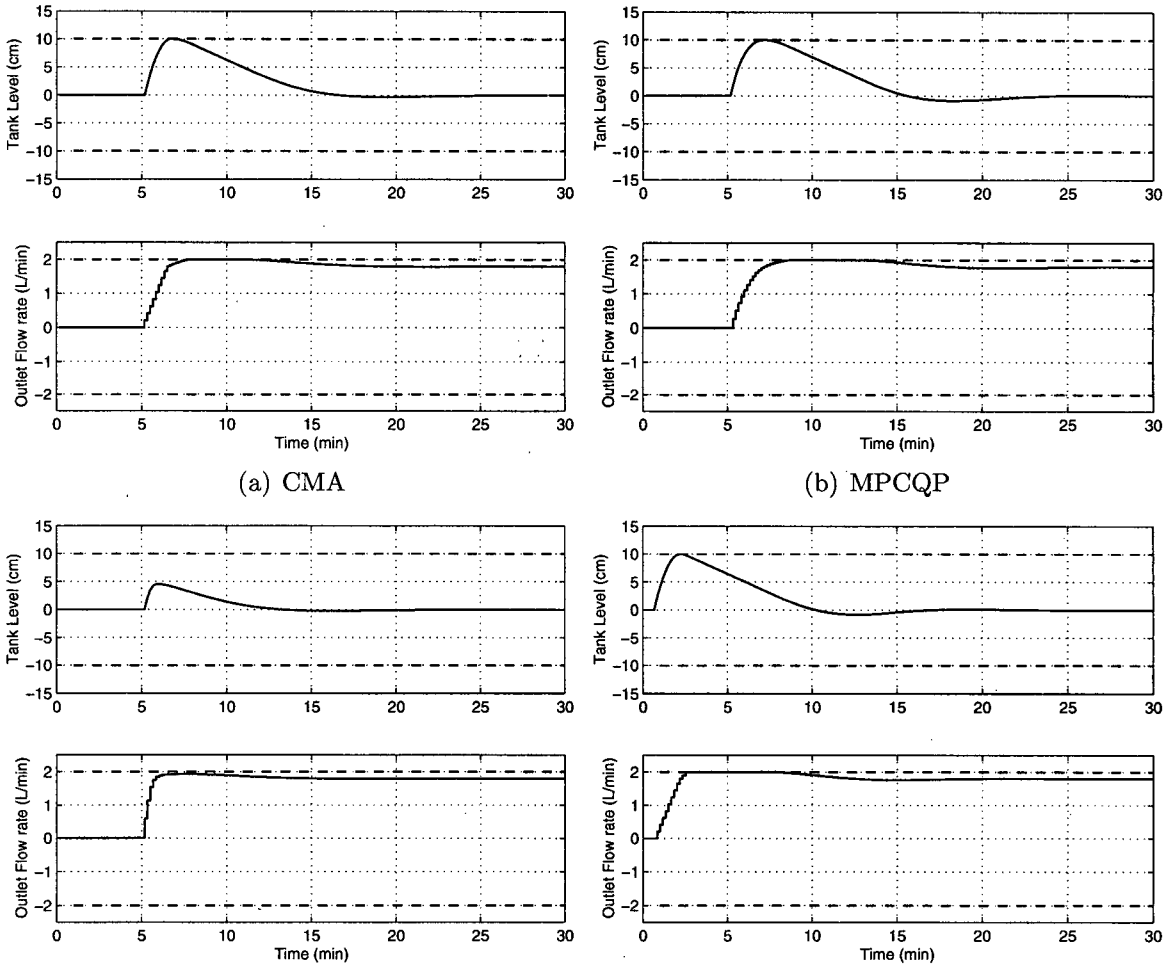

(a) CMA (b) MPCQP

(c) CMN (d) $\mathcal{L}_1/\mathcal{L}_\infty$ MPC

Figure 4.2: Controller comparison: Single tank with level and flow rate constraints

The $\mathcal{L}_1/\mathcal{L}_\infty$ MPC algorithm is able to maintain both the tank level and the flow rate within its limits. Furthermore, the controller is able to effectively utilize the surge capacity to attenuate the flow disturbance. The outlet flow in Figure 4.2(d) increases in the optimal ramp. This result shows a significant improvement over the CMN algorithm when flow rate constraints are active. This further concludes that the original CMN formulation was sensitive to tuning, refer to Conjecture 3.1. The MRCO values for each controller are listed in Table 4.2. The $\mathcal{L}_1/\mathcal{L}_\infty$ MPC algorithm is able to produce the optimal MRCO value, similar to the CMA algorithm. This is not surprising as both algorithms are explicitly minimizing the MRCO as their optimization objectives. In conclusion, for the single tank system, $\mathcal{L}_1/\mathcal{L}_\infty$ MPC is able to provide excellent results in the presence of both level and flow rate constraints.

Next the multivariable case is studied. Again, the two-tank system is used for comparison and the simulations are set up according to parameters listed in Table 3.6 with actuator constraints of ± 2 L/min. Figure 4.3 and Figure 4.4 show the multivariable

results for recycle fractions of 40% and 70%, respectively. Even though both tanks are utilized for flow filtering, the solution is not MRCO optimal as listed in Table 4.3. It is a significant improvement, but the MPCQP still outperforms both LP-based controllers.

	MRCO (L/min/min)	
Controller	$f_1 = f_2 = 40\%$	$f_1 = f_2 = 70\%$
MPCQP	1.34	0.69
CMN	3.69	3.65
$\mathcal{L}_1/\mathcal{L}_\infty$ MPC	1.80	1.41
MRCO Optimal	0.99	0.56

Table 4.3: MRCO: Two tank system with level and flow rate constraints

It is interesting to note that MPCQP is able to provide the lowest MRCO and provides smooth control actions. On the other hand, the $\mathcal{L}_1/\mathcal{L}_\infty$ MPC algorithm steers the tank levels using very nonsmooth control actions. The explanation behind such behaviour is explored in the next section in an attempt to better understand MPCQP and $\mathcal{L}_1/\mathcal{L}_\infty$ MPC algorithms .

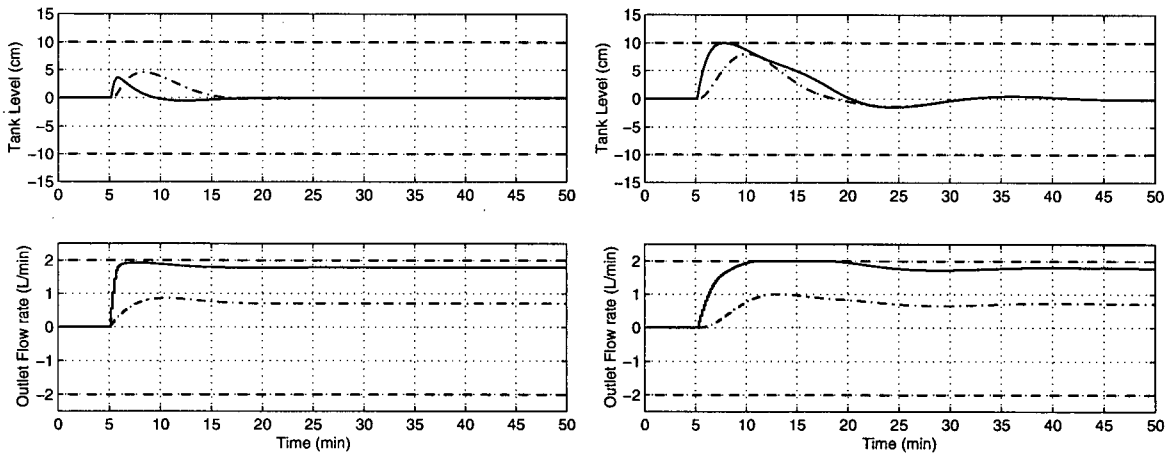

(a) CMN (b) MPCQP

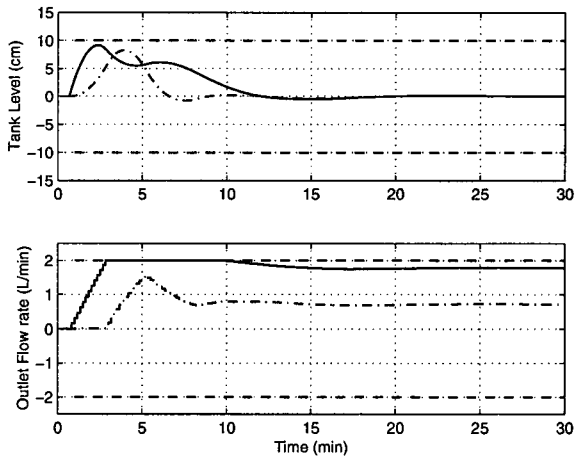

(c) $\mathcal{L}_1/\mathcal{L}_\infty$ MPC

Figure 4.3: Controller comparison: two-tank system with level and flow rate constraints for $f_1 = f_2 = 40\%$, Tank 1 (solid) Tank 2 (dash-dot)

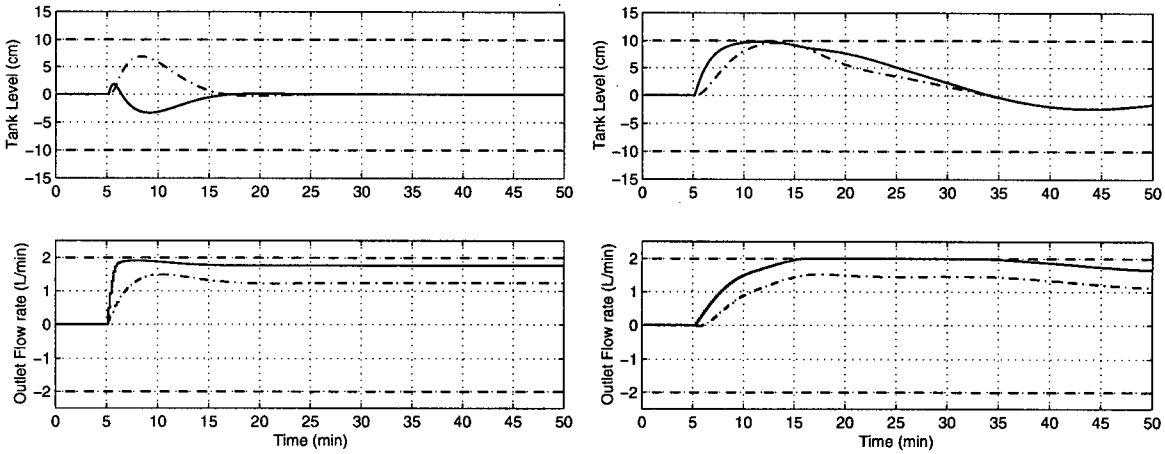

(a) CMN (b) MPCQP

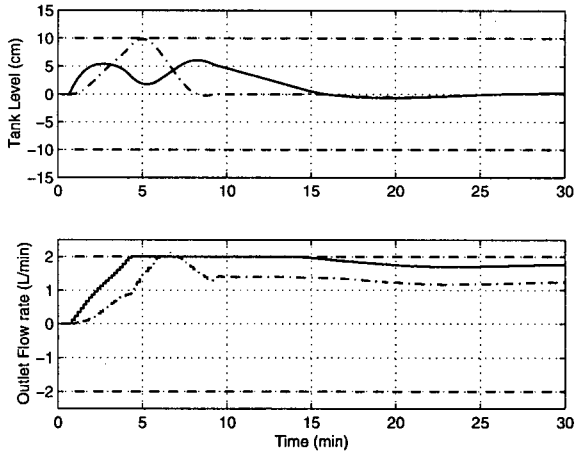

(c) $\mathcal{L}_1/\mathcal{L}_\infty$ MPC

Figure 4.4: Controller comparison: two-tank system with level and flow rate constraints for $f_1 = f_2 = 70\%$, Tank 1 (solid) Tank 2 (dash-dot)

4.3 LP vs. QP Optimization for MPC

In section 4.1, a novel formulation for MPC using LP was devised. Despite removing the restrictive terminal constraints, $\mathcal{L}_1/\mathcal{L}_\infty$ MPC exhibited some very nonsmooth closed-loop dynamics. The reason for such behaviour is not solely associated with defining the MPC cost function; it is also associated with using LP optimization [4]. It is well known that the solution to an LP problem always lies at an intersection of constraints. Therefore, even in the unconstrained case, the MPC solution using LP is on the constraint boundary that is defined by the control objective and system constraints. Furthermore, the cost function defined using the $\mathcal{L}_p$ norm, where $p = 1 \text{ or } \infty$, is nonsmooth with a discontinuity at the origin [4]. This discontinuity generally does not allow an analytical solution even in the unconstrained case, whereas minimization with respect to the $\mathcal{L}_2$ norm, using MPCQP formulation, has an analytical solution in the unconstrained case, and when the active constraints are known [15].

In the receding horizon implementation of MPC, the optimization is performed at each sampling time. As can be seen in equation (4.3), the constraint set is a function of state feedback and previous control actions. The constraint set is not static but dynamically updated via feedback. Hence the optimal control policy can shift in an erratic manner as the constraint set shifts. This observation can be seen in both Figure 4.3 and Figure 4.4. It can be seen that the control actions are in ramp fashion which suggests that the ∇U values are identical from one iteration to the next for the duration of each ramp. It can be postulated that there exists a polyhedron or a feasible set on the constraints that serves as the optimal set, resulting in identical ∇U, until the constraint set is shifted by feedback and another optimal set becomes active. Then the new value of ∇U continues to be optimal until the constraint set shifts again resulting in a ramp control action of a different slope. This indeed is the case in LP optimization [19], [16]. As the right-hand side of equation (4.3) is perturbed in the neighborhood of $\mathtt{b}$, the solution continues to be in the same feasible set or polyhedron with a given basis. However, when $\mathtt{b}$ is perturbed beyond a threshold value, the feasible set shifts giving rise to a new basis. The new basis can be far from the previous one, resulting in an abrupt change in the optimal solution. However, the QP optimization does not exhibit such behaviour.

The aforementioned description can be illustrated using Figure 4.5. In this simple example, the LP and QP optimization contours, along with their constraint sets which define the feasible region, are shown. In Figure 4.5, the optimal solution for LP exists at point A, the intersection of constraints which has the smallest cost. The optimal solution to the QP problem is in the centre of the ellipses and away from constraints. For ease of explanation, assume that in the receding horizon implementation using feedback, the constraint set is rotated clockwise. In the LP case, the optimal solution will continue to be

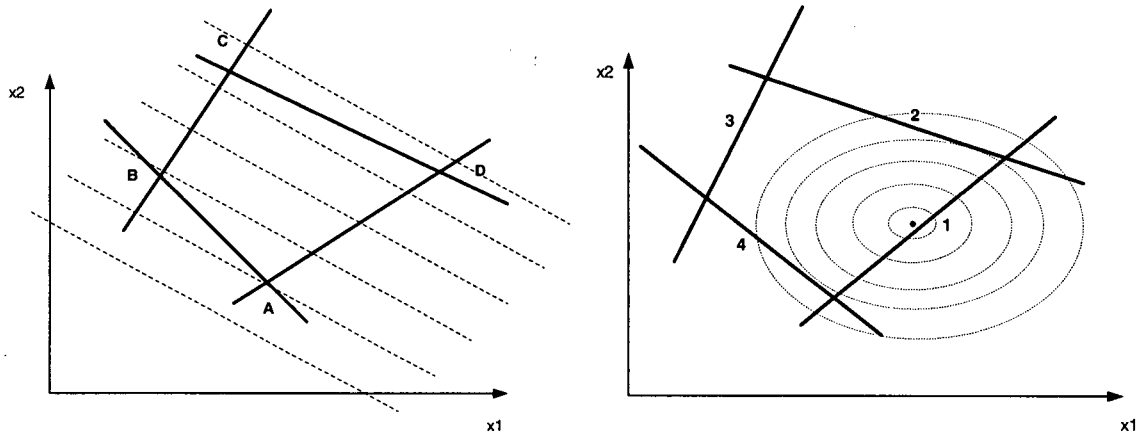

(a) LP (b) QP

Figure 4.5: Cost contours and binding constraints

at point A as the rotation progresses at each sample time. This occurs until the moment when the cost associated with point D becomes lower than the cost associated with point A, where the solution will jump from A to D and the basis for the optimal solution will change. This type of nonsmoothness in the control action leads to the closed-loop behaviour observed in the LP formulation of MPC. In the QP case, the origin will continue to be the optimal solution until line segment 2 starts to cut across the origin. During such a situation the optimal solution would ride smoothly along the active constraint without jumping to another constraint or a constraint intersection.

Chapter 5

Real Time Implementation

In Chapter 3 it was shown through simulation studies that the CMA algorithm was very well suited for a single tank system. In the MIMO case, it was demonstrated that the MPCQP algorithm gave excellent results in minimizing the MRCO and handling system constraints. A major drawback of the numerical algorithms is the high computational demand for real-time applications. It was also demonstrated in Chapter 3 that the Decoupled CMA algorithm provided excellent results.

In this chapter the CMA algorithm for the single tank and Decoupled CMA for the two-tank system are presented are validated on the two-tank system.

5.1 Instrumentation & Control System Setup

The general setup of the two-tank system was discussed in section 1.2.2. In this section, the instrumentation and control system setup are described.

The outlet flow rate of each tank is measured using an Omega FTB2000 series flow sensor, capable of measuring up to $5\,L/min$. The square wave frequency output of the flow sensor was converted to $0-10$ volts using an Omega iDRN signal conditioner. Water is removed from each tank using a constant speed 360 PROVEN pump with a maximum flow rate of $4\,\mathrm{L}/min$ and the outlet flow rate is controlled using a Honeywell Q7230 electric actuated control valve. The level is measured using a Flowline level sensor. Figure 5.1 shows the calibration of the flow and level sensors.

The computer control system was set up to utilize a dSpace real-time digital signal processing (DSP) board for data acquisition and controller implementation. The control algorithms were implemented in Matlab using Real-Time Workshop, along with dSpace hardware and software. The level control strategy was implemented in a cascade configuration. A local flow controller, executed every half second, served as the inner loop. The outer loop consisted of a level controller executed every four seconds. Under this configuration, the supervisory level controller dictates the flow rate setpoint for the lower level flow controller. The flow controller accommodates the valve/flow nonlinearities and linearizes the system for the level controller. The inner loop, flow controller, is executed every 0.5 seconds while the outer loop level controller is executed every 4 seconds.

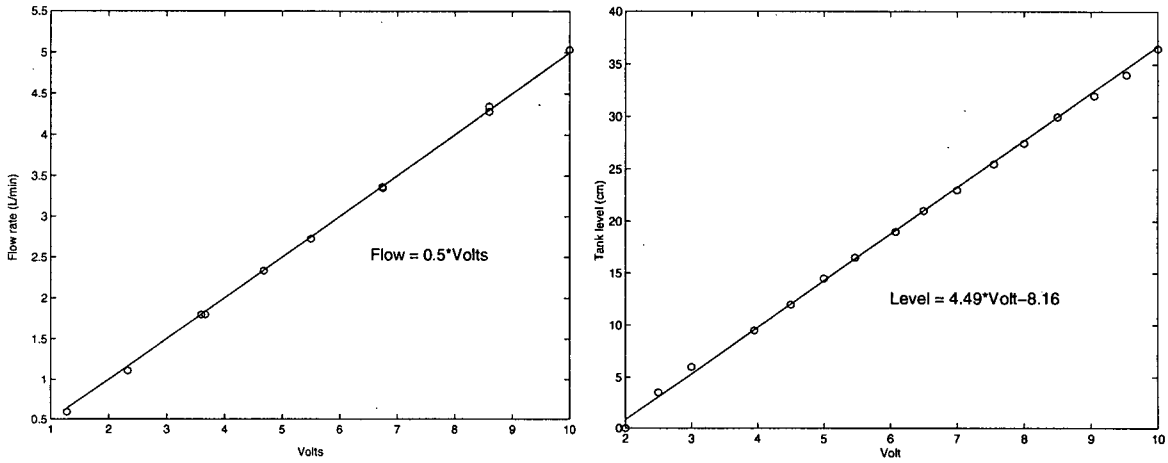

(a) Flow sensor (b) Level Sensor

Figure 5.1: Flow sensor and level sensor calibrations

5.2 Controller Implementation

The control algorithm complexity is of great concern in all real-time applications. The host computer must compute the control action within the allocated time. Even though the MPCQP algorithm provided the best compromise between constraint handling and flow smoothing, the MPCQP solution could not be implemented due to a lack of computational power and hardware setup. This illustrates the major disadvantage of MPC based on QP optimization. Likewise, using LP for optimization was too demanding within MatLab.

5.2.1 Single Tank System

The CMA algorithm has an analytical solution and therefore a very low computational demand. The results of the CMA implementation are compared with the PI algorithm. The controllers were tuned as per described in section 3.2.1 in the unconstrained case. The implementation parameters were set up according to Table 5.1.

Nominal Level	15.0 cm
Minimum level constraint	5.0 cm
Maximum level constraint	25.0 cm
Minimum flow rate constraint	0.0 L/min
Maximum flow rate constraint	4.0 L/min

Table 5.1: Single tank implementation parameters

The implementation results are displayed in Figure 5.2. For the given load disturbance, the PI controller was not able to maintain the tank level within constraints. In fact, the level increased until it overflowed the tank. Fortunately, the tank was equipped

with an overflow drain pipe which prevented water from spilling onto the laboratory floor. The PI controller makes very small changes to the outlet flow rates which are not adequate to maintain the level within constraints. The CMA algorithm, however, is aware

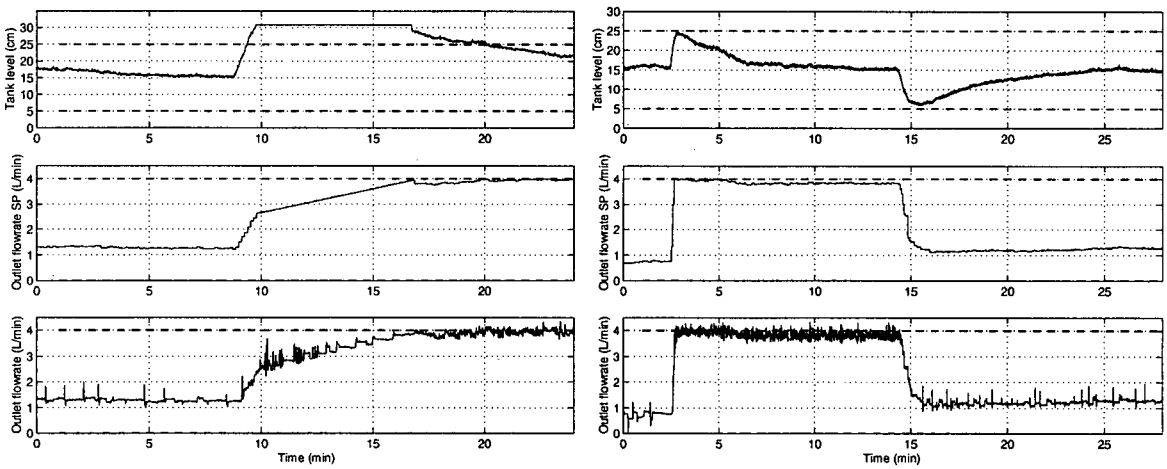

(a) PI (b) CMA

Figure 5.2: Controller comparison: single tank real time implementation

of level constraints and, thus, manipulates the outlet flow rate appropriately. The second load disturbance for the CMA controller was of lower magnitude and, as a result, a much more linear control action is observed. Also, during the second load disturbance, the rate of change of the manipulated variable was smaller than the first, again indicating that the controller is aware of level constraints. The real-time implementation of CMA agrees with the simulation results as the level is brought back to setpoint in about $3.0N_u$ or 9 minutes. This demonstrates that the CMA algorithm is extremely powerful and can be easily implemented.

5.2.2 Two Tank System

In the MIMO case, the Decoupled CMA algorithm was implemented on the two-tank system. Figure 5.3 shows the implementation results. In the laboratory two-tank system, the recycle flow fractions were functions of the outlet flow rates. As the outlet flow rate from each tank is manipulated for level control, the recycle flow fraction, assumed to be fixed in simulation, varies significantly. As the recycle flow fraction changes, the two-tank system model also changes. The flow fraction from each tank was calculated off-line and implemented in real-time using the corresponding outlet flow rate as the scheduling variable.

The control objectives for each tank were as stated in Table 5.1. A load disturbance was introduced into Tank 1, similar to the MIMO simulations. During the first load

disturbance, the inlet flow rate to Tank 1 is cut back. This forces the Tank 1 level to drop, but due to the decoupling strategy the Tank 2 level is not significantly effected. The small deviations observed are a result of an imperfect decoupling matrix due to recycle fraction changes and plant/model mismatch. Both tank levels and outlet flow rates are maintained within their limits. A second load disturbance was introduced into to Tank 1 at about 18 minutes. In that scenario, the recycle fraction was higher. Also, due to the lack

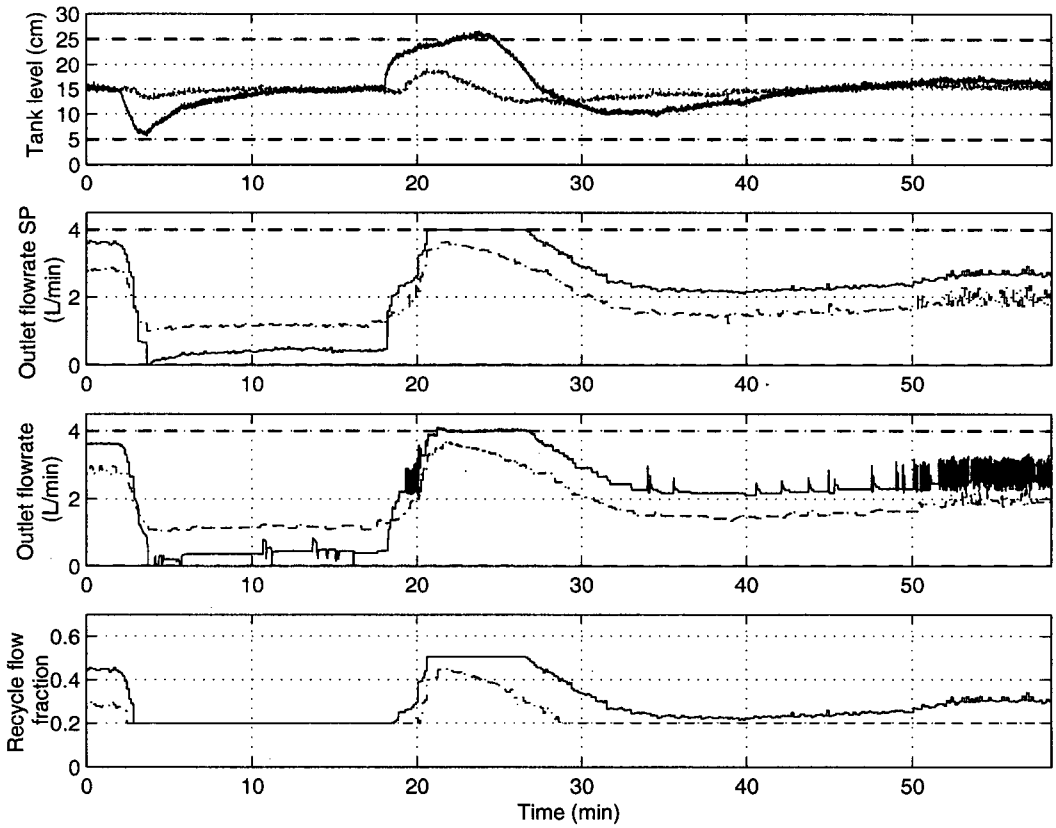

Figure 5.3: Decoupled CMA: two-tank system real time implementation, Tank 1 (solid) Tank 2 (dash-dot)

of perfect decoupling, the deviations in the Tank 2 level were greater. It can also be seen that the outlet flow rate of Tank 1 saturated for about 8 minutes. During saturation, only partial decoupling can be achieved resulting in level constraint violation. The observation in simulations that increasing the recycle fraction also increases closed-loop settling times was confirmed. Even under the circumstances of not having a perfect decoupling matrix and limited control authority, the Decoupled CMA algorithm performed quite well.

Chapter 6

Conclusions and Future Work

The objective of this thesis was to investigate the multivariable averaging level control problem. An industrial pulp pressure screening system served as a motivation for the thesis. In order to conveniently study the problem, a two-tank system that mimicked the industrial system was constructed. System model equations were derived based on the laboratory two-tank system.

From the controllability analysis, it was determined that the system is controllable provided the recycle flow fraction is less than unity. RGA analysis indicated that as the recycle fractions increase, the off-diagonal elements of the RGA increase significantly. This indicates that the process is highly coupled and multivariable controller design is required.

In the SISO system (zero recycle fraction), various controller design techniques were considered. The PI control algorithm was discarded due to its inability to handle level constraints. It was concluded that the CMA algorithm with an anti-windup circuit provides MRCO optimal results. A theorem was developed that proves CMA is the optimal control policy in the SISO case. Therefore, strategies based on numerical optimization are not needed in this case.

In the multivariable case, the fundamental disturbance assumption of the CMA algorithm was violated due to coupling in the process. As a result, the Decentralized CMA controller was unable to handle level constraints. Therefore, decentralized control is not sufficient for the MIMO averaging level control problem.

It was shown that the multiple tank system possesses a special structure that allows the multivariable model to be split into dynamic and static components. This led to the construction of a constant decoupling matrix that decouples the system across all frequencies. A theorem was developed stating that the Decoupled CMA is guaranteed to handle level constraints provided flow rate constraints are not encountered. In this case, decoupled control provides excellent results, and furthermore the analytical solution is practically attractive. However, one drawback is that not all the available surge capacity is used for flow filtering. Therefore, Decoupled CMA can never be MRCO optimal. Furthermore, when limited control authority is available, the Decentralized CMA is no longer able to perfectly decouple the system and hence violation of level constraints may result. Therefore, decoupled control only works well in the situation where control authority is not a limiting factor.

In order to ensure that both level and flow rate constraints are satisfied, full mul-

tivariable control is required. The ability to handle all process constraints comes with an increased computational demand as a numerical solution must be implemented. It was shown that the MPC cost function can be set up to penalize either the $\mathcal{L}_2$ or $\mathcal{L}_\infty$ norm of the control actions. The minimization with respect to the $\mathcal{L}_\infty$ norm of ∇u provides the potential for MRCO optimal control as MRCO is explicitly minimized. While penalizing the $\mathcal{L}_2$ norm of ∇u can never achieve the optimal minimum MRCO, the algorithm has other desirable properties.

The CMN algorithm was able to handle both level and flow rate constraints. However, the algorithm is sensitive to tuning. It was shown through simulations that the CMN controller became short-sighted, causing the terminal constraints to compete with the flow smoothing objective. It was conjectured that the prediction horizon that achieves MRCO optimal control is a function of constraints, process coupling and disturbance magnitude. In industry, the disturbance magnitude is usually unknown, and the process operating point and constraints can be changed by the operator depending on the demands in the plant. Hence, tuning a controller that requires such precise information about the plant can be extremely difficult and impractical. The CMN can be tuned to provide MRCO optimal control provided the prediction horizon is increased. A very long prediction horizon can be problematic as the controller will take much longer to bring the tank level back to setpoint. If the level is far from setpoint for an extended period of time, another disturbance in the same direction can lead to disastrous results.

In order to alleviate the problem of short-sightedness due to terminal constraints, a novel mixed-norm MPC formulation was presented. An attractive feature of the $\mathcal{L}_1/\mathcal{L}_\infty$ MPC is that the terminal constraints are removed and integral action is achieved by minimizing the absolute value of the control error. In addition, the MRCO continues to be explicitly minimized, and the strategy still utilizes LP optimization. This was compared to a more conventional MPC implementation based on minimizing a quadratic index and QP optimization (MPCQP). $\mathcal{L}_1/\mathcal{L}_\infty$ MPC provided a significant improvement over CMN algorithm and both $\mathcal{L}_1/\mathcal{L}_\infty$ MPC and MPCQP proved to be insensitive to tuning. But for the given simulation scenario, MPCQP provided the lowest MRCO. Although, theoretically, $\mathcal{L}_1/\mathcal{L}_\infty$ MPC formulation should ultimately provide the minimum MRCO in the general case, practically speaking there is very little to choose between the algorithms. The final choice would likely depend on implementation issues such as; computational complexity, storage requirements and the ability to customize the optimization algorithms.

It was observed that when MPC was formulated to utilize LP instead of QP optimization, the control increments were piece-wise constant. This nonsmooth behaviour was determined to be associated with the change in basis of the LP solution, as the constraint set is modified during the receding horizon MPC implementation. The solution can shift

from one basis to another abruptly, leading to nonsmooth control actions. A MPC formulation that uses QP can have a solution away from the constraints and does not switch abruptly when constraints become active, thus leading to smoother control actions.

The PI and CMA algorithms were implemented in real-time on a single tank and the simulation results were validated. In the MIMO case, the MPCQP was computationally too demanding for the computer system to be implemented in real-time. The Decoupled CMA algorithm, having an analytical solution, was implemented. Again the real-time results agreed with simulation studies. On the two-tank system it was found that the flow fraction was a function of the outlet flow rate. The flow rate was used as the scheduling variable to update the decoupling matrix in real-time, which further showed the versatility of the Decoupled CMA.

This thesis leads to some interesting questions which could be explored in the future. In the multivariable framework, the existence of an analytical solution similar to CMA could be sought. This would greatly decrease the computational demand as no on-line optimization would be required. The condition that determines the critical prediction horizon length in the CMN could also be investigated. In the Decoupled CMA strategy, the saturation of one actuator results in partial decoupling. In such a situation there is still one degree of freedom available, namely the second actuator. The control action applied to the second actuator should be recalculated to improve process decoupling. This can be achieved by developing and utilizing an appropriate simultaneous correction algorithm.

Nomenclature

$\bar{r}$	Future setpoint vector, $\Re^{pN_2,1}$, equation (2.21)
$\hat{A}$	Augmented state transition matrix, $\Re^{n+p,n+p}$, equation (2.17)
$\hat{B}$	Augmented input matrix, $\Re^{n+p,m}$, equation (2.17)
$\hat{C}$	Augmented observation matrix, $\Re^{p,n+p}$, equation (2.17)
$\mathbb{M}$	Input constraint stacking matrix, equation (2.22)
$\mathbb{N}$	State constraint stacking matrix, equation (2.25)
$\mathcal{A}$	MPC reduced equation matrix: constant, equation (2.21)
$\mathcal{B}$	MPC reduced equation matrix: varying, equation (2.21)
$\mathcal{C}$	Augmented prediction observation matrix, $\Re^{pN_2,pN_2}$, equation (2.21)
$\mathcal{D}$	Constraint set matrix for MPCQP: fixed, equation (2.27)
$\mathcal{E}$	Constraint set matrix for MPCQP: varying, equation (2.27)
$\mathcal{F}$	Augmented free response prediction matrix, $\Re^{(n+p)N_2,n+p}$, equation (2.18)
$\mathcal{G}$	Augmented forced response prediction matrix, $\Re^{(n+p)N_2,mN_u}$, equation (2.18)
$\mathcal{H}$	Summing matrix, equation (2.29)
$\mathcal{I}$	Past input matrix, equation (2.23)
$\mathcal{K}$	Terminal constraint forcing matrix in CMN, see page 27
$\mathcal{M}$	Enforces N_2^{th} error minimization, equation (4.2)
$\mathcal{Q}$	Augmented output weight matrix, $\Re^{pN_2,pN_2}$, equation (2.21)
$\mathcal{R}$	Augmented input weight matrix, $\Re^{mN_u,mN_u}$, equation (2.21)
$\mathcal{U}$	Close set of all admissible controls, page 15
$\mathcal{X}$	Independent cost function term, equation (2.20)
N	Ceiling operator, see equation (2.4)
A	Constraint matrix in LP optimization: Constant

b	Right hand side matrix in LP: Varying
c	LP cost function matrix
x	LP optimization vector
$\widetilde{A}$	Constant spatial matrix, equation (2.10)
A	State transition matrix, $\Re^{n,n}$, equation (1.4)
A_c	Tank cross-sectional area (cm), equation (1.1)
B	Input matrix, $\Re^{n,m}$, equation (1.4)
C	Observation matrix, $\Re^{p,n}$, equation (1.4)
D_d	State disturbance matrix, $\Re^{n,m}$, equation (1.4)
f	Recycle flow fraction, equation (1.1)
G_c	Controller transfer function, see page 16
G_d	Disturbance transfer function, equation (1.3)
G_{PI}	PI controller, equation (2.9)
G_p	Process transfer function, equation (1.3)
I	Identity matrix
$k(s)$	Process dynamics, equation (2.10)
$k^\star$	Number of samples for level constraint to become active, see equation (2.4)
K_c	PI controller gain, equation (2.9)
l_{max}	Maximum input slew rate constraint, equation (2.24)
l_{min}	Minimum input slew rate constraint, equation (2.24)
m	Number of inputs
M_δ	Maximum deviation from setpoint
m_{max}	Maximum input constraint, equation (2.22)
m_{min}	Minimum input constraint, equation (2.22)
n	Number of states

N_1 Initial prediction horizon, equation (2.11)

N_2 Final prediction horizon, equation (2.11)

n_{max} Maximum state constraint, equation (2.25)

n_{min} Minimum state constraint, equation (2.25)

N_u Control prediction horizon, see equation (2.5)

$N_u^{\dagger}$ Critical prediction horizon, see equation (2.7)

p Number of outputs

Q Output weight, equation (2.11)

q Outlet flow rate (L/min), equation (1.1)

R Input weight, equation (2.11)

r Tank level setpoint (cm), page 14

s Laplace Transform variable, equation (1.3)

T Sampling time, see page 1.2.3

T_r PI controller reset time, equation (2.9)

t_s Settling time

U Future control actions, $\Re^{mN_u,1}$, see page 20

u Outlet flow rate (L/min), equation (1.1)

u^0 Unconstrained solution of CMA, see equation (2.5)

$u^{\star}$ Constrained solution of CMA, see equation (2.6)

u_{max} Maximum flow rate constraint (L/min), equation (2.2)

u_{min} Minimum flow rate constraint (L/min), equation (2.2)

$V_{\nabla u}$ Cost function: minimization with respect to ∇u, equation (2.11)

W Decoupling matrix, see page 17

W_c Controllability matrix, see page 10

W_o Observability matrix, see page 10

x System state variable, equation (1.4)

y Tank level, equation (1.1)

y_{lim} Tank level constraint, h_{max} or h_{min}, (cm), page 14

y_{max} Maximum tank level constraint (cm), page 14

y_{min} Minimum tank level constraint (cm), page 14

z^{-1} Z-transform variable, equation (2.9)

Greek Letters

α Minimum input constraint matrix, equation (2.22)

β Maximum input constraint matrix, equation (2.22)

δ Maximum sate constraint matrix, equation (2.25)

γ Minimum state constraint matrix, equation (2.25)

Λ Integration matrix, equation (2.23)

μ Chebyshev approximation variable in CMN, equation (2.29)

Ω Flow imbalance, see equation (2.3)

ω Maximum input slew rate constraint matrix, equation (2.24)

ψ Minimum input slew rate constraint matrix, equation (2.24)

Ξ Augmented state prediction, $\Re^{(n+p)N_2,1}$, equation (2.18)

ξ Augmented state vector, $\Re^{n+p,1}$, equation (2.13)

Vector Norms

$\mathcal{L}_1$ Sum-norm: $\| x \|_1 = | x_1 | + \cdots + | x_n |$

$\mathcal{L}_2$ Euclidean norm: $\| x \|_2 = \sqrt{x_1^2 + \cdots + x_n^2}$

$\mathcal{L}_\infty$ Chebychev norm: $\| x \|_\infty = \max_i | x_i |$

Mathematical Symbols

∇ Difference operator, see equation (2.5)

$\Re$ Euclidean space of all reals

$\mathbf{0}$ Matrix of zeros

$\mathbf{1}$ Column vector of ones, see equation (2.29)

Abbreviations

CMA Campo & Morari's Analytical solution

CMN Campo & Morari's Numerical algorithm

CSTR Continuous stirred tank reactor

DRIP Dual range integral/proportional

LOC Limited output change

LP Linear programming

LQ Linear quadratic

MIMO Multi-input multi-output

MPC Model based predictive control

MRCO Maximum rate of change of the outlet flow rate

OPC Optimal predictive controller

PID Proportional-Integral-Derivative

PL Proportional-lab

QP Quadratic programming

RC Ramp controller

RGA Relative gain array

SISO Single-input single output

SSE Sum of squared error

References

[1] Ari Ammala. *Fractionation of Thermomechanical pulp in pressure screening.* Phd thesis, University of Oulu, 2001.

[2] M. Khanbaghi B. Allison, R. Harper. Optimal averaging level control for surge tanks. *IEEE APC 2001 Workshop*, 2001.

[3] E.H. Bristol. On a new measure of interactions for multivariable process control. *IEEE Trans. Automt. Contr.*, 11:133–134, 1966.

[4] J.B. Rawlings C.V. Rao. Linear programming and model predictive control. *Journal of Process Control*, 10:283–289, 2000.

[5] V. Manousiouthakis D.D. Sourlas. Best achievable decentralized performance. *IEEE Transactions on Automatic Control*, 40(11):1858–1871, 1995.

[6] C. Bordons E.F. Camacho. *Model Predictive Control.* Springer-Verley, London, 1999.

[7] M.E. Salgado G.C. Goodwin, S.F. Graebe. *Control System Design.* Prentice-Hall Inc., New Jersey, 2001.

[8] M. Huzmezan. *Theory and aerospace applications of constrained model based predictive control.* Phd thesis, Cambridge University, 1998.

[9] J. Paris J.C. Bonhivers, M. Perrier. Model predictive control for integrated management of whitewater tanks. *Tappi J.*, Nov. 2002.

[10] W. Fehervari J.P. Shunta. Nonlinear control of liquid level. *Instru. Tech.*, 23(43), January 1976.

[11] T.Y. Kuc K. Park, G. Choi. Wiener-hopf design of the optimal decoupling control system with state-space formulas. *Automatica*, 38:319–326, 2002.

[12] T.J. McAvoy K.A. McDonald. Model predictive optimal averaging level control. *AIChE Annual Meeting*, 1984.

[13] J.D. Kelly. Tuning digital pi controllers for minimal variance in manipulated input moves applied to imbalanced systems with delay. *Can. Jour. of Con.*, 76:967–973, October 1998.

[14] S. Skogestad M. Hovd, R. Braatz. Optimality of svd controllers. *Technical Report*, 1996.

[15] J.M. Maciejowski. *Predictive Control with constraints.* Pearson Education Ltd., England, 2001.

[16] K. Ritter M.J. Best. *Linear Programming: active set analysis and computer programs.* Prentice-Hall Inc., London, 1985.

[17] M.W. Foley M.S. Sidhu, K.W. Kwok. Minimum variance optimal pi controller for averaging level control: an industrial application. *IEEE APC Workshop 2001*, 2001.

[18] B.R. Copeland M.W. Foley, K.E. Kwok. Polynomial lq solution to he averaging level control problem. 16^{th} *International conference on CAD/CAM, Robotics and Factories of the Future, Port of Spain, Trinidad W. I.*, June, 2000.

[19] W. Murray P.E. Gill, M.H. Wright. *Practical Optimization.* Academic Press, London, 1981.

[20] M. Morari P.J. Campo. Model predictive optimal averaging level control. *AIChE J.*, 35(4):579–597, April 1989.

[21] G. Dumont M. Davies S. Ogawa, B.J. Allison. A new approach to averaging level control. *IEEE CDC*, 2002.

[22] W.L. Luyben T.F. Cheung. A further study of the pl level controller. *ISA Trans.*, 18(2), 1979.

[23] P.S. Buckley W.L. Luyben. A proportional-lag level controller. *Instrumentation Tech.*, 65, 1977.